Plant Cell Reports (2024) 43:108
https://doi.org/10.1007/s00299-024-03174-2

ORIGINAL ARTICLE

Capsicum chinense Jacq.-derived glutaredoxin (*CcGRXS12*) alters redox status of the cells to confer resistance against pepper mild mottle virus (PMMoV-I)

R. M. Saravana Kumar[1,2] · S. V. Ramesh[3] · Z. Sun[5] · Sugitha Thankappan[4] · Naga Prafulla Chandrika Nulu[6] · Asish Kanakaraj Binodh[7] · Sundaravelpandian Kalaipandian[2,6] · Ramachandran Srinivasan[8]

Received: 18 October 2023 / Accepted: 12 February 2024 / Published online: 1 April 2024

Abstract

Key message **The *CcGRXS12* gene protects plants from cellular oxidative damage that are caused by both biotic and abiotic stresses. The protein possesses GSH-disulphide oxidoreductase property but lacks Fe–S cluster assembly mechanism.**

Abstract Glutaredoxins (Grxs) are small, ubiquitous and multi-functional proteins. They are present in different compartments of plant cells. A chloroplast targeted Class I *GRX* (*CcGRXS12*) gene was isolated from *Capsicum chinense* during the pepper mild mottle virus (PMMoV) infection. Functional characterization of the gene was performed in *Nicotiana benthamiana* transgenic plants transformed with native *C. chinense GRX* (*Nb:GRX*), *GRX*-fused with GFP (*Nb:GRX-GFP*) and *GRX*-truncated for chloroplast sequences fused with GFP (*Nb:Δ2MGRX-GFP*). Overexpression of *CcGRXS12* inhibited the PMMoV-I accumulation at the later stage of infection, accompanied with the activation of salicylic acid (SA) pathway pathogenesis-related (PR) transcripts and suppression of JA/ET pathway transcripts. Further, the reduced accumulation of auxin-induced Glutathione-S-Transferase (pCNT103) in *CcGRXS12* overexpressing lines indicated that the protein could protect the plants from the oxidative stress caused by the virus. PMMoV-I infection increased the accumulation of pyridine nucleotides (PNs) mainly due to the reduced form of PNs (NAD(P)H), and it was high in *Nb:GRX-GFP* lines compared to other transgenic lines. Apart from biotic stress, *CcGRXS12* protects the plants from abiotic stress conditions caused by H_2O_2 and herbicide paraquat. CcGRXS12 exhibited GSH-disulphide oxidoreductase activity in vitro; however, it was devoid of complementary Fe–S cluster assembly mechanism found in yeast. Overall, this study proves that *CcGRXS12* plays a crucial role during biotic and abiotic stress in plants.

Keywords Pepper mild mottle virus—Italian strain (PMMoV-I) · Glutaredoxin (GRX) · Pyridine nucleotides (PNs) · Glutathione-S-Transferase (GST) · Glutathione (GSH) · Pathogenesis related (PR)

Introduction

Plant virus invasion subjugates the host machinery to express viral genes and induces oxidative stress conditions (Akbar et al. 2020; Wang et al. 2021). Plants manifest different strategies to stop the spread of virus such as the development of hypersensitive response (HR) (Balint-Kurti. 2019), *R*-gene-mediated resistance (Palukaitis and Yoon 2020), silencing of viral genes (Wang et al. 2012; Ismayil et al. 2018) and RNA decay (Li and Wang 2019). Apart from *R*-gene-mediated resistance, many other plant-derived genes also protect the plants from viral infection by controlling the oxidative damage, caused by the pathogen. Exploring the functions of the differentially expressed host genes during the plant–pathogen interaction provides a better comprehension of plant genes-mediated resistance, and it also helps in designing a novel plant-protection strategy (Marmonier et al. 2022). In this current study, pepper mild mottle virus—Italian strain (PMMoV-I) belonging to *Tobamovirus* genus, causing serious economic loss to pepper crops (*Capsicum chinense*), was used to study the role of host-derived genes against virus infection. Through mRNA differential display PCR and RACE-PCR, a cDNA fragment corresponding to class I Glutaredoxin (*CcGRXS12*) gene was isolated from

Communicated by Prakash Lakshmanan.

Extended author information available on the last page of the article

C. chinense plants during the compatible (PMMoV-I) and incompatible (PMMoV-S) viral infection.

Glutaredoxins (GRXs) are small, ubiquitous, and low molecular weight oxido-reductases, sharing the structural features of thioredoxin family of proteins, and they are conserved among prokaryotes and eukaryotes (Holmgren 1995). The number of GRXs reported in the photosynthetic organisms is found to be high and they are classified into six classes. Class I (C1, C2, C3, C4, and C5/S12 subgroup), Class II (S14, S15, S16, and S17) and Class III (21 CC-type in Arabidopsis) are relatively well characterized, while other classes warrant further studies (Couturier et al., 2010; Couturier et al. 2009a). Individual class of GRX proteins has different catalytic activities and specific functions; thus, various plant-derived GRXs coordinate different functions. Class I GRXs reduce the protein–protein disulphide bonds and protein–glutathione disulfide bonds by utilizing GSH as reductants (Rouhier et al. 2007). Class II GRXs reduce protein–glutathione disulphide bonds by utilizing ferredoxin-thioredoxin reductase (FTR) as their reducing equivalent supplier (Zaffagnini et al. 2008). The oxidoreductase property of the GRXs enables the protein to take part in many redox-dependent pathways, causing various protein activation/deactivation.

Recent studies have revealed the importance of GRXs during plant–pathogen interactions. GRXs contribute to the susceptibility of plants to necrotrophic pathogens, while their effect in response to biotrophic pathogens is distinctly different. Salicylic acid (SA)-induced CC-type GRXs (GRXC9/ROXY19 and GRXS13/ROXY18) have been identified as contributors to susceptibility to the necrotrophic pathogen *B. cinerea* (Ndamukong et al. 2007; La Camera et al. 2011). This susceptibility is attributed to the over-accumulation of H_2O_2. Similarly, the overexpression of CC-type glutaredoxins in rice and Arabidopsis (ROXY1, ROXY2) leads to an accumulation of H_2O_2, enhancing plants' susceptibility to *B. cinerea* (Wang et al. 2009). In a study by Yang et al. (2022), it was demonstrated that overexpression of *GsGRX4* renders plants susceptible to *B. cinerea* by accumulating H_2O_2 and suppressing both JA content and JA-related marker genes. A member of the tomato CC-type GRX family (*SlGRXC6*) has been shown to reduce the accumulation of tomato leaf curl virus (TLCV) by interacting with the virus protein (Zhao et al. 2021). In addition, overexpression of the rice Class I GRX (*OsGRX20*) has been found to mediate resistance against bacterial blight caused by *Xanthomonas oryzae* pv. *oryzae* (Xoo) (Ning et al. 2018)..

Phytohormonal pathway activation plays critical roles during the pathogen attack, plant growth and developments (Ma and Ma 2016; Bozbuga et al. 2022). During pathogen attack, systemic acquired resistance (SAR) is developed at the distal part of the infection site (Fodor et al., 1997), which is concomitant with the activation of various phytohormone pathways and accumulation of the corresponding pathogenesis-related (PR) proteins (Van Loon and Van Strien 1999). In general, resistance to biotrophs is mediated through SA pathway activation, while jasmonic acid/ethylene (JA/ET) pathway acts in response to necrotrophs. Thus, plants have the ability to regulate the phytohormonal pathways based on the type of pathogen it encounters. Activation of SA pathway during the pathogen attack suppresses the JA and auxin-dependent defense pathways (Vlot et al. 2009; Yang et al. 2015; Yuan et al. 2017). Different phytohormones induces the expression of GRXs (Yang et al. 2021; Sharma et al. 2013; Herrera-Vásquez et al. 2015; El-Kereamy et al. 2015; Malik et al. 2020) suggesting that GRXs transmit the information to activate phytohormonal pathway.

In the SA/JA signal transduction pathway, several transcription factors (TGA, ORA59) and proteins act as signaling components. GRX activates/deactivates the signaling components through its oxidoreductase property. In the NPR1-TGA transducing system, reduction of the co-activator (NPR1) and the transcription factor (TGA) occurs prior to their interaction. Following the NPR1-TGA interaction, the TGA protein binds to its cognate promoter element (as-1) of PR gene's promoters and mediates the transcription of PR genes (Després et al. 2000). Salicylic acid-induced GRX480 suppresses the expression of JA induced PDF1.2 by interacting with TGA2 factor (Ndamukong et al. 2007). In Arabidopsis, 17 of the 21 CC-type GRXs are known to interact with TGA2 factor (Zander et al. 2012), implying that this molecular interaction is an inevitable process. Apart from pathogen attack, many developmental activities are also influenced by the TGA:GRXs interactions (Gutsche et al. 2017; Ehrary et al. 2020; Ruan et al. 2018, 2022; Li et al. 2019; Uhrig et al. 2017). Glutaredoxins activate the TGA factor through post-translational modification (Hou et al. 2019). Activation of SA pathway inhibits the expression of JA/ET-induced genes, through the repression of ORA59 (Pre et al. 2008; Van der Does et al. 2013). CC-type GRXs were reported to suppress the ORA59 activation (Zander et al. 2012). Apart from acting as transducing element, GRXs influence the biosynthesis of phytohormones (El-Kereamy et al. 2015). In addition, GRXs are actively engaged in the Fe–S cluster assembly mechanism (Lu 2018).

In the present study, the functional characterization of *CcGRXS12* gene was carried out by overexpressing in *N. benthamiana* Domin. Innately, these plants are susceptible to PMMoV-I viral infection. However, the plants showed recovery from PMMoV-I infection at later stage when the gene was overexpressed. This recovery phenomenon helps in obtaining molecular insights into the resistant mechanisms, conferred by *CcGRXS12* during plant–virus interaction. The indispensable roles of GRX in the activation of phytohormone pathways were studied by analyzing the accumulation of corresponding PR transcript(s). The role of *CcGRXS12* in

altering the redox status of the cell was deciphered by analyzing the accumulation of oxidized and reduced forms of pyridine nucleotides (PNs). In addition, this study deduced the role of *CcGRXS12* in plant abiotic stress tolerance and Fe–S cluster assembly mechanism.

Materials and methods

Plant materials and virus inoculation

Capsicum chinense N.J. Jacq. PI159236 (L^3L^3) and various *N. benthamiana* Domin transgenic plants were maintained in growth chambers at 32 °C with 16 h of photoperiod (16 h of light and 8 h of dark), light intensity of 8000 lx and 70% relative humidity. For viral inoculation, first pair of the developed leaves from the plants was mechanically inoculated with purified virions at a concentration of 50 µg/mL in inoculation buffer (0.02 M sodium phosphate buffer, pH 7.0), using carborundum as an abrasive. At 7 days post-inoculation (dpi), samples were taken from inoculated and systemic leaves; at 14 and 21 dpi, samples were collected from systemic leaves; and at 28 dpi, samples were collected from the asymptomatic (recovered leaves) along with the symptomatic leaves.

Viral strain, purification, and viral RNA extraction

Pepper mild mottle virus—Italian strain (PMMoV-I) was used in this study (Wetter et al. 1984). The protocols for purification of virion and viral RNA extraction were followed as described by Alonso et al. (1991) and Garcia-Luque et al. (1990).

Isolation of *CcGRXS12* and sequence analysis

Previously, "mRNA differential PCR" identified the *Capsicum chinense* (L^3L^3) (PI 159236)-derived transcript corresponding to *GRX* gene when the plants were infected with compatible (PMMoV-I) and incompatible (PMMoV-S) viral strains. The complete sequence of the gene was obtained through RACE-PCR (Chenchik et al. 1998). The chloroplast targeting region of the protein was predicted by chloroP 1.1 program (Emanuelsson et al. 1999). Protein sequence alignment was performed by Clustal W program (http://www.ebi.ac.uk/Tools/msa/clustalw2/).

Measurement of oxidoreductase activity

The GSH-disulfide oxidoreductase activity of the purified native protein (CcGRXS12) was determined using the Hydroxyethyl disulfide (HED) assay (Holmgren and Aslund 1995). For expression in a prokaryotic system, a truncated CcGRXS12 protein (63 amino acids in length) with a 6X His-tag at its N-terminal region was cloned into the pQE-1 vector (obtained from Dr. Maria Teresa). The gene insert was confirmed through sequencing. *E. coli* M15 (pREP4) strain was transformed with the plasmid harboring the cloned gene construct. Protein expression and purification was performed using His-select Nickel affinity gel resin column (Sigma Aldrich, USA) according to the manufacture's instruction. GRX activity was measured as an oxidation of NADPH in a reaction comprising 1 mM GSH, 0.7 mM β-hydroxy ethyl disulphide (HED), 0.25 mM NADPH and 6.4 µg/mL glutathione reductase in Tris–Cl pH 7.4. The reaction mixture was incubated at room temperature for 2 min then the decrease in OD at 340 nm was recorded in a spectromax micro-plate reader for 1 min at room temperature. The decrease in absorbance at 340 nm, following the addition of His-GRX protein, was recorded. Enzyme activities were normalized by correcting for the absorbance prior to the addition of GRX protein. One unit of activity is defined as the consumption of 1 µmol of NADPH per minute calculated from the expression $(\Delta A340 \times V)/(\min \times 6.2)$, where V is the cuvette volume in ml and 6.2 is the mM extinction coefficient for NADPH. Three independent experiments were performed at each substrate concentration, and the apparent K_m value and K_{cat} values were calculated by non-linear regression using the program SigmaPlot 12.0.

Transgenic plants

Nicotiana benthamiana Domin transgenic plants constitutively expressing free GFP (*Nb:GFP*; line 11), full-length GRX (*Nb:GRX*; line 3), full-length GRX fused with GFP (*Nb:GRX-GFP*; line 16) and chloroplast targeting region truncated GRX (63aa) fused with GFP (*Nb:Δ2MGRX-GFP*; line 40) were analyzed. These transgenic lines were obtained from Dr. Maria Teresa Serra Yoldi (Montes-Casado et al. 2010). The constructs were driven at their N-terminus by CaMV35S promoter and have NOS terminator at its C-termini.

Plant total protein extraction

Total protein from fresh leaf samples (1 mg) was extracted using 5 µL of Laemmli buffer (Laemmli 1970). In brief, the samples were heated to 95 °C for 5 min, followed by sonication for 5 min, and then clarified by centrifugation at 20,000*g* for 5 min. Total protein extracts (5 µL) were resolved in SDS polyacrylamide gels (SDS-PAGE) using 17.5% and 4.5% polyacrylamide as solving and concentrating gels, respectively, according to Laemmli (1970).

Viral coat protein analysis

Total plant protein extracts (5 µL) and a viral coat protein extracts of 5, 2.5 and 1.25 ng were electrophoresed on 17.5% and 4.5% SDS-PAGE gel. The proteins were stained with Coomassie Blue R-250 and PMMoV-I coat protein was quantified using a densitometer and the Quantity One 1-D analysis software (Bio-Rad, Hercules, USA).

Immunoblot analysis

Total proteins profiled in SDS-PAGE were electrotransferred onto PVDF membranes (Amersham). The membranes were initially blocked with PBST (3.2 mM Na_2HPO_4, 0.5 mM KH_2PO_4, 1.3 mM KCl, 135 mM NaCl, and 0.05% Tween 20, pH 7.2) containing 5% skimmed milk for 30 min. For the immunodetection of GRX, GFP and viral coat protein (CP), the electro transferred membranes were incubated overnight at 4 °C with the specific antisera of His-GRX (1/1000; raised in our lab), GFP-specific polyclonal antibody (1/250; Santa Cruz Biotechnology, INC.) and PMMoV-I CP (1/1000; raised in our lab). Detection of antigen–antibody complexes was carried out with peroxidase-conjugated goat anti-rabbit IgG (GARPO) (Nordic) at 1/5000 dilution. The immunoreaction was visualized with ECL chemiluminescence kit (GE Healthcare Amersham) as per manufacturer's instructions. The enzymatic reaction produces a luminescent compound that is detected by visible-light sensitive films (Hyperfilm, Pharmacia).

Protoplast infection assay

Protoplasts were obtained from the four different *N. benthamiana* transgenic lines as described by Ruiz del Pino et al. (2003) with minor modifications. Protoplasts were washed for couple of times with ice-cold solution containing 12% mannitol and 6 mM $CaCl_2$. Protoplasts were counted and adjusted to the concentration of 1.3×10^6 protoplasts/mL using ice-cold electroporation buffer (12% mannitol, 6 mM $CaCl_2$, 80 mM KCl, and pH 7.2). For protoplasts infection, 4×10^5 protoplasts in a final volume of 300 µL were taken in a 0.2 cm electroporation cuvette along with 20 µg of PMMoV-I RNA and kept on ice. For transformation, a single pulse of 0.12 kV and 125 µF was applied with a Gene Pulser (Bio-Rad laboratories, Hercules, CA) immediately after addition of 20 µg of viral RNA. Following the pulse, the protoplasts were kept on ice for 20 min and diluted in CPW-M13. Later, centrifuged at 80 × g for 5 min and diluted to 5×10^5 protoplasts/mL in CPW-M13 and incubated at 25 °C under dark. Protoplasts were harvested at 16, 24 and 48 h with a short spin at 134 g, and a couple of washing in mannitol buffer and the resultant protoplast was re-suspended in 5X Laemmli buffer. The viral infection was detected by Western blot method using PMMoV-I coat protein-specific antibody.

Sub-cellular localization studies of CcGRXS12 protein

For analyzing the sub-cellular localization of CcGRXS12 protein, protoplasts obtained from the different GFP expressing transgenic lines (*Nb:GFP*, *Nb:GRX-GFP* and *Nb:Δ2MGRX-GFP*) were fixed with 4% formaldehyde in 9% mannitol (pH 7.2). To label the nuclei, DAPI staining was performed. In brief, protoplasts (10^4) were incubated with 100 µL of 2 µg/mL DAPI solution in PBS-9% mannitol for 5 min. To that 900 µl of PBS-9% mannitol was added and kept for another 15 min, and then the protoplasts were collected and washed with PBS-9% mannitol for twice and finally suspended in 100 µL PBS-9% mannitol. Around 20 µL of this sample was loaded over poly-L-lysine-coated glass slides for visualization. For compartmentalization study, autofluorescence from chlorophyll and DAPI staining at nuclei were analyzed. Different fluorescent signals were detected at specific wavelengths [GFP detection at 550 nm (excitation 580 nm), chlorophyll autofluoresence at 540 nm (excitation 600 nm) and DAPI at 610 nm (excitation at 650 nm)] using a TCSP Leica microscope.

RNA isolation and probe preparation

Total leaf RNA was extracted according to the method prescribed by Chomczynski and Sacchi (1987) using TRIzol reagent and then followed the manufacturer's instruction with a minor modification. Briefly, additional centrifugation at 12,000 g for 10 min at 4 °C after plant tissue homogenization and an additional final RNA precipitation step with 0.3 M sodium acetate pH 5.2 and 2.5 volumes of 100% ice-cold ethanol for overnight were performed. The digoxigenin-labeled RNA probes were prepared using the linearized plasmids harboring various gene products according to the instructions described in MAXIscript kit manual. The cloned gene products, for preparing the riboprobes, include salicylic acid pathway marker proteins (PR1, PR-2a and PR5), the JA/ET pathway marker protein (PR-2d) and the gene for auxin inducible Glutathione-S-Transferase (GST) (pCNT103) (obtained from Carmen Castresana), and the clone pT-CPS containing the 593 bp from PMMoV-S CP (Gilardi et al. 1998).

Northern blot hybridization

For Northern blot analysis, RNA samples (10 µg) were denatured at 65 °C for 4 min in MOPS-Acetate-EDTA buffer (20 mM MOPS, 15 mM sodium acetate, 3 mM EDTA, pH 7.0) in the presence of 10% formamide, 0.9% formaldehyde,

and 0.06 mg/mL ethidium bromide. Subsequently, the samples were electrophoresed on 1.5% agarose-formaldehyde gels containing MOPS buffer (50 mM MOPS, 0.4 mM EDTA, pH 7) and 6% formaldehyde, using MOPS electrophoresis buffer under a current of 5 V/cm. After visualization under UV light, the RNAs were transferred to nylon membranes (Hybond-N, Pharmacia), following the protocol described in Sambrook et al. (1989), and fixed by irradiation with UV light (120 mJ) using a UV Stratalinker apparatus (Cultek). The membranes, with transferred RNA, were stored under cold conditions for later use.

For hybridization with digoxigenin-labeled RNA probes, the membranes were incubated with standard buffer (5xSSC, 0.1% sodium-lauroylsarcosine, 0.02% SDS and 2% blocking reagent, blocking reagent is provided by manufacturer) for 2 h at 65 °C. Then, the membranes were hybridized overnight at 68 °C with specific RNA probes in standard buffer containing 100 ng of the corresponding probe. After hybridization, the membranes were washed twice in (2 × SSC solution and 0.1% SDS) for 15 min each at room temperature (RT) and twice in (0.1 × SSC and 0.1% SDS) for 15 min at 65 °C. Probe detection was performed using the DIG luminescent detection kit (Roche, Penzberg, Germany) according to manufacturer's protocol. In brief, membranes were incubated in blocking solution of maleic buffer (0.1 M Maleic acid and 0.15 M NaCl) containing 1% blocking reagent for 30 min, then in anti-digoxigenin alkaline phosphatase conjugated antibody at 1:10,000 for 30 min followed by washing twice in washing buffer. After equilibration in detection buffer, membranes were incubated with chemiluminescent substrate CSPD and exposed to X-ray sensitive films (Hyperfilm, Pharmacia) for 30 min.

Measurement of pyridine nucleotide (PN) contents

Pyridine nucleotide contents in the mock and PMMoV-I-infected plants at 28 dpi were analyzed by grinding 30 mg of fresh leaf sample with ball bearings and centrifuged for 12,000*g* for 1 min. The supernatant obtained was used for selective extraction of NAD(P)H in acid medium and NAD(P)+ in alkaline medium (Hajirezaei et al. 2002). The samples were neutralized to the final pH of 8.0 to 8.5 and made as 100 µl aliquots and frozen at − 80 °C for further analysis. PNs in the neutralized extracts were determined following Gibon et al. (2004). Statistical difference was analyzed by SAS 9.1 program (SAS 9.1 Inc. 2004) using one-way analysis of variance (ANOVA).

Abiotic stress tolerance assay

Role of *CcGRXS12* in abiotic stress tolerance was studied by growing various *N. benthamiana* transgenic plants in one-half MS media in the presence and absence of both 3 mM H_2O_2 and 1 µM paraquat. The seedlings were grown horizontally for the first 3 days and then they were grown in vertical position for another 1 week. Root length was measured after 10 days. The experiments were performed in triplicates of 30 seedlings each and repeated thrice. The seedlings were grown at 25 °C and 16 h of photoperiod. Statistical analyses were performed by SAS 9.1 program (SAS 9.1 Inc. 2004) using one-way analysis of variance (ANOVA).

Heterologous expression of *CcGRXS12* in *S. cerevisiae*

To clone and express CcGRXS12 mature protein in yeast cells, pGEM-T easy vector (pGEM-GRX), harboring the full-length *CcGRXS12* gene was used. Gene-specific primers were designed to amplify the full-length gene excluding the chloroplast targeting region. In order to prevent codon breakage while expression in yeast, the 'g' nucleotide (small letter) introduced immediately after the *Not*I site in the forward primer (5´-ATAAGAATGCGGCCGCgTCGGGTTCA TTCGGGTCC-3´) so as to introduce genetic code for alanine at the end of the mitochondrial targeting region. The reverse primer (5´-GAAGATCTGCTTTCTGTTTTTCCA GGATTA-3´) had an overhang of *Bgl*II site. The amplified fragment was cloned in to pMM221 vector (obtained from Dr. E. Herrero, Universitat de Lleida, Lleida, Spain) which contains the yeast mitochondrial targeting sequence at its 5′ end and 3HA/His6 tag at its 3′ end (Molina-Navarro et al. 2006). The resultant plasmid containing the *CcGRXS12* gene sequence was transformed into yeast *Δgrx5* mutants, and the selection of the transformants was performed following Rodriguez-Manzaneque et al. (1999).

Growth conditions of *S. cerevisiae*

The yeast strains employed in this study, namely wild type (W303-1B; WT), *Δgrx5* mutant (MML100; *Δgrx5*) and yeast *GRX5* expressing in *Δgrx5* mutants (MML240; *Δgrx5/GRX5*), were already reported in Rodriguez-Manzaneque et al. (1999) and the *CcGRXS12* transformed in yeast *Δgrx5* mutant strain (*Δgrx5/CcGRXS12*) (in this work). All yeast strains were grown in YPD, respiratory defective YPG and SC media as mentioned in Rodríguez-Manzaneque et al. (2002). For oxidant sensitive assay, the above-mentioned yeast strains were grown in the media containing 0.3 mM tert-butyl hydroperoxide (t-BOOH) and 1.25 mM diamide (Sigma Aldrich, USA) in a serial dilution of 1:10 and incubated for 3 days.

CcGRXS12 in Fe–S cluster assembly mechanism

Role of *CcGRXS12* in Fe–S cluster assembly mechanism was studied by analyzing the accumulation level of free iron

(Fish 1988), and measuring the relative ratio of aconitase to malate dehydrogenase activity (Robinson et al. 1987) for the aforementioned yeast strains.

Results

Sequence features of *Capsicum chinense* glutaredoxin

Sequence analysis of *Capsicum chinense* glutaredoxin gene (*CcGRX)* shows that the ORF comprises 531 bp which codes for 177 amino acids. Protein sequence analysis revealed the presence of CSYS active site which is the characteristics of class I / S12 GRXs. Based on the analysis, the isolated gene was named as *CcGRXS12*. Sequence alignment of the isolated GRX with the well-characterized poplar GRX (PtGRXS12) (Coutruier et al. 2011) protein showed that apart from CSYS active site, other motifs such as ELD, TVPN, GG and second cysteine were found to be conserved (Fig. 1a).

CcGRXS12 possesses GSH-disulfide oxidoreductase activity

Mature form of the CcGRXS12 protein (114 aa) without the chloroplast targeting region was cloned in pQE1 vector and expressed in M15 (pREP4) *E. coli* system. Purification of native protein was carried out using nickel affinity column. The predicted molecular mass and pI for the protein

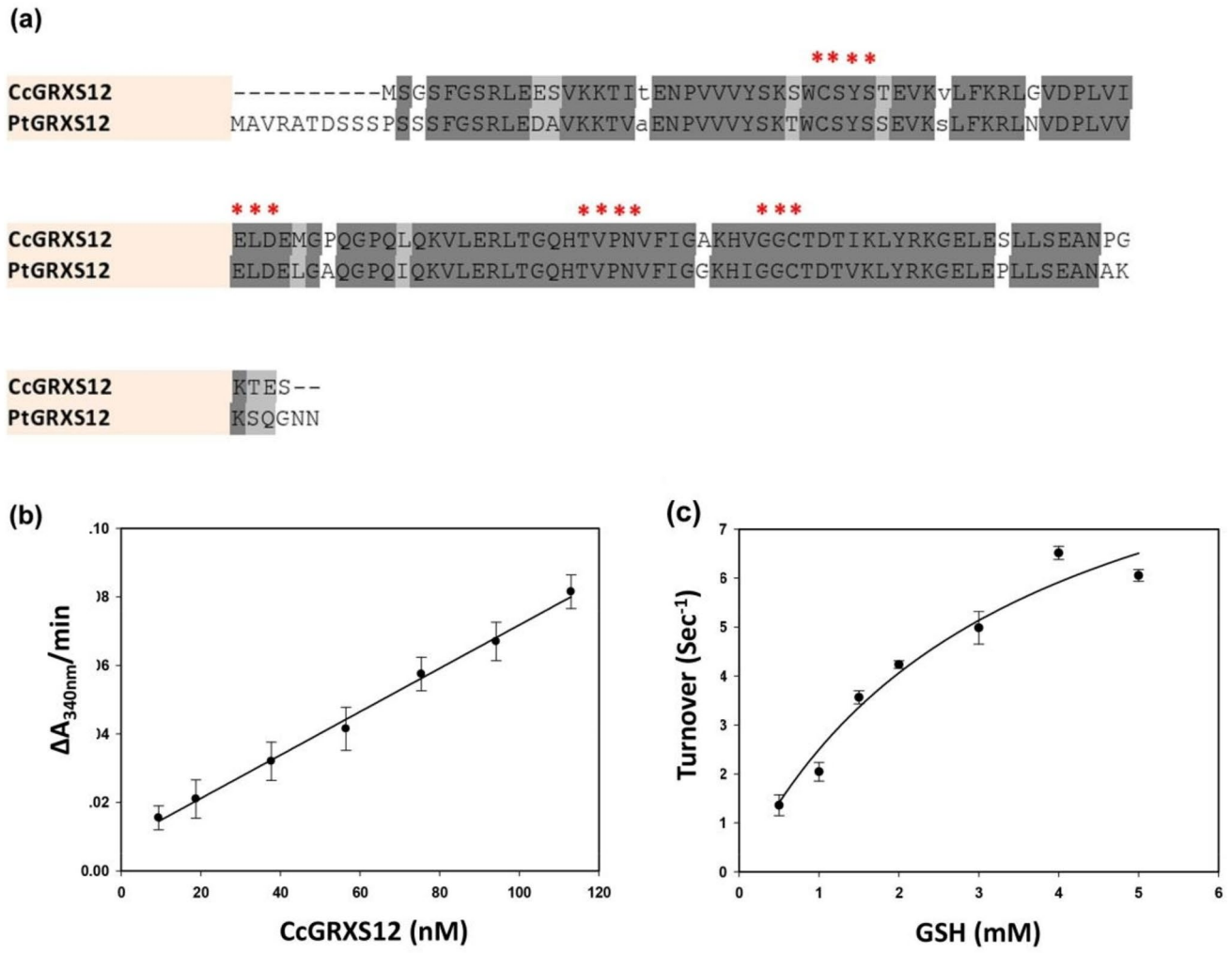

Fig. 1 **a** Comparative protein sequence alignment of isolated GRX (CcGRXS12) with GRX characterized from Poplar (PtGRXS12). Sequence features have shown that the conserved CSYS active site, and there are several conserved regions between these two proteins. **b** Linear dependence of HED activity on *Cc*GRXS12 concentration is expressed as ΔA_{340}/min. **c** Variations of the apparent turnover during hydroxyethyl disulphide (HED) assay were calculated by varying concentrations of GSH (0.5–5 mM). The data represent mean ± S.D. The best fit was obtained using the Michaelis–Menten's equation using non-linear regression analysis

were 13.8 kDa and 8.24, respectively. Specific activity of the protein (0.12 U/nM) was calculated by varying the concentration of His-CcGRXS12 from 10 to 125 nM by keeping a constant GSH concentration (1 mM) (Fig. 1b). The correlation kinetics between the protein and GSH was measured by keeping the protein concentration at 84 nM and varying the GSH concentration from 0.5 to 5 mM (Fig. 1c). The apparent K_m (4.9 ± 1.9 mM) and apparent turnover K_{cat} (14.63 ± 4.8 s^{-1}) values were calculated using the Michaelis–Menten equation and the catalytic efficiency value (K_{cat}/K_m (M^{-1} s^{-1})) was found to be 3.05×10^3. In vitro assay showed that CcGRXS12 protein participates in deglutathionylation reaction.

Selection and analysis of *CcGRXS12* overexpressing lines

For investigating the functional role of GRX, several *N. benthamiana* transgenic plants overexpressing various form of *CcGRXS12* were used as described in "Materials and methods". The gene constructs developed and utilized for the genetic transformation of *N. benthamiana* are illustrated in Fig. 2a. The transgenic plants were grown in a media containing high concentration of kanamycin. The expression level of the gene in the T3 transgenic plants were analyzed by Western blot method (Fig. 2b). Analysis showed that the expression of *CcGRXS12* in *Nb:GRX-GFP* lines was found to be ~ 10 times higher than the other two *CcGRXS12* overexpressing lines. Phenotypic analysis reveals that *Nb:Δ2MGRX-GFP* lines showed stunted growth and wide leaf surface area when compared to free *GFP* and other *CcGRXS12* overexpressing lines.

Sub-cellular localization of *CcGRXS12*

To investigate the in vivo sub-cellular localization of *CcGRXS12*, expression of *GFP*-fused *CcGRXS12* gene was studied in the protoplasts of various transgenic lines including *Nb:GFP*, *Nb:GRX-GFP* and *Nb:Δ2MGRX-GFP* using confocal microscope. The fluorescence of the native GRX-fused GFP superimposed with chloroplast while the free GFP expressing line (*Nb:GFP*) and the line overexpressing the truncated form of the GRX-fused GFP (*Nb:Δ2MGRX-GFP*) showed expression signal throughout the cytoplasm and nuclei (Fig. 3a). These results confirmed that CcGRXS12 is targeted to the chloroplast and the N-terminus amino acids (63 in number) are essential for the protein to localize in chloroplast. Western blot analysis with GRX- and GFP-specific antibodies showed that the GRX expression in the transgenic lines were GFP-fused one (Fig. 3b).

Overexpression of *CcGRXS12* inhibits PMMoV-I accumulation

A time-course study (7, 14 and 28 dpi) on viral coat protein (CP) titres in the control and *GRX* overexpressing transgenic

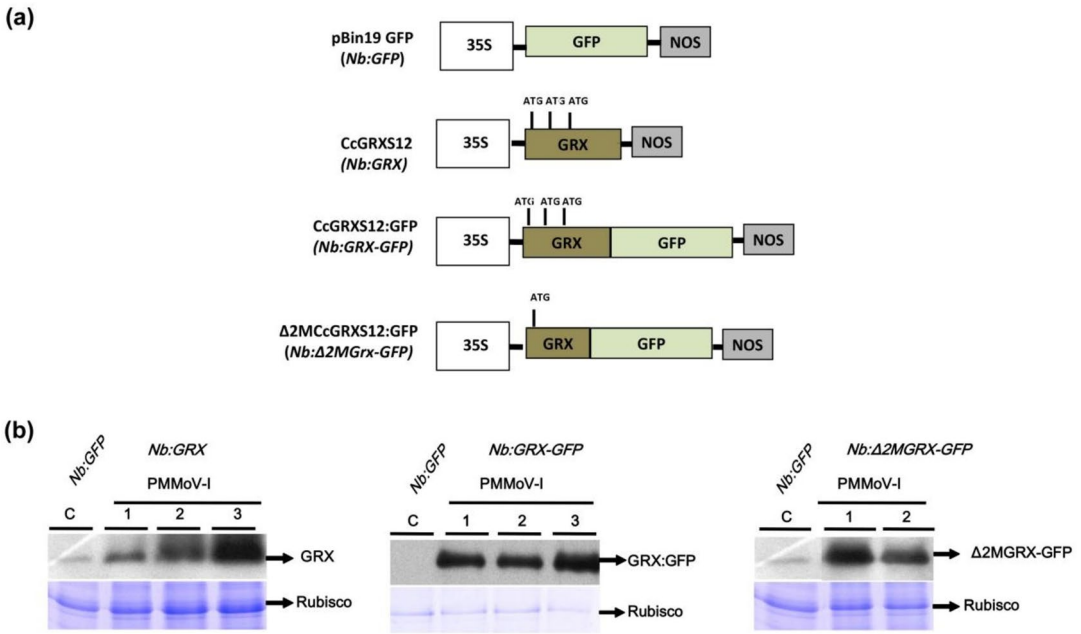

Fig. 2 **a** Various gene constructs harboring GRXs used for the transformation of *N. benthamiana* plants, and the resultant transgenic lines are mentioned in the parenthesis. b Western blot analysis of CcGRXS12 expression in the upper leaves of *N. Benthamiana* from virus-infected transgenic lines. The protein extracts from *Nb:GRX-GFP* are diluted 10 times when compared with other lines. Lower panels show Coomassie staining of total proteins as a loading control

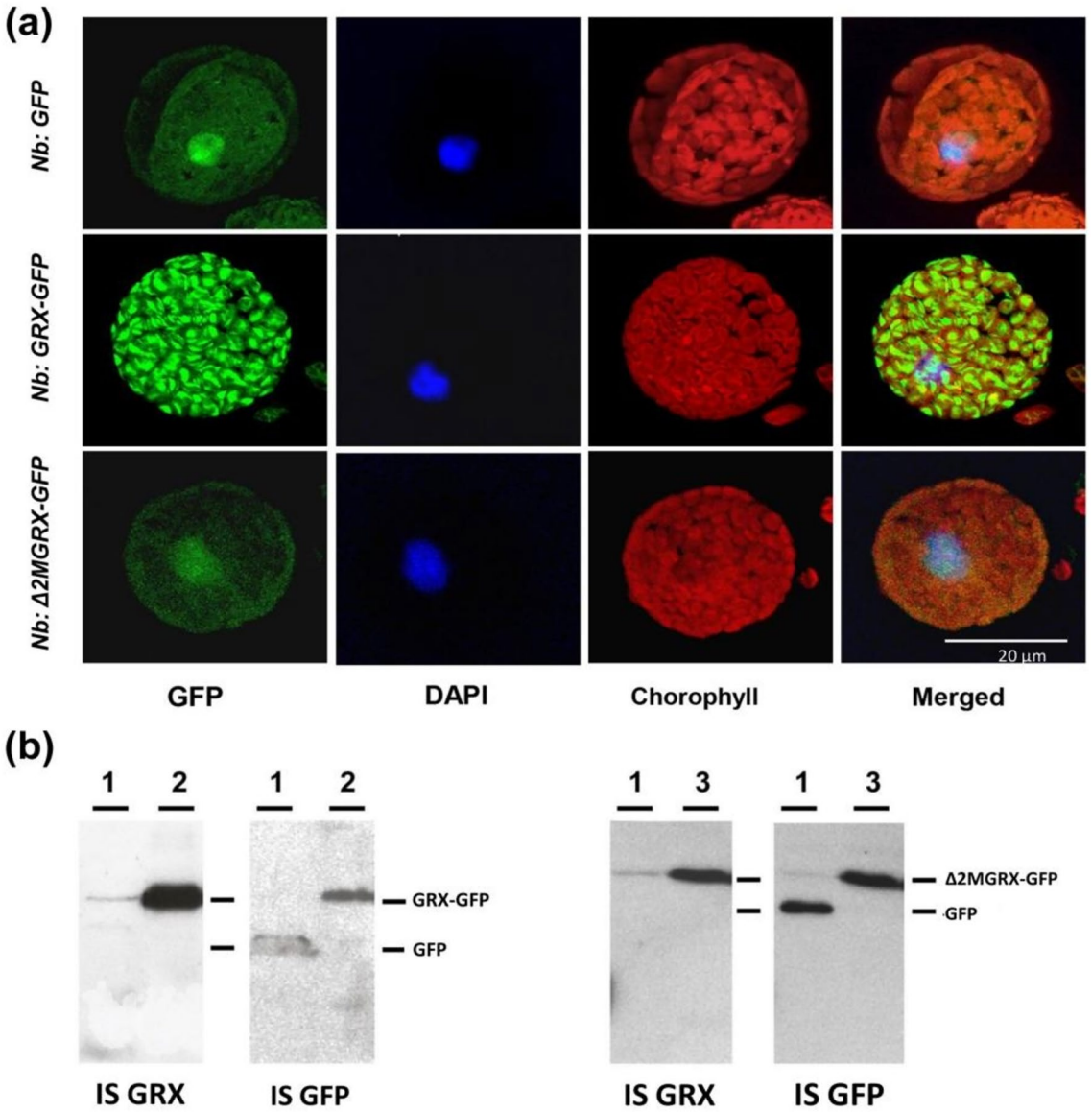

Fig. 3 **a** Confocal microscopic study of *CcGRXS12* in *N. benthamiana* protoplast obtained from various transgenic lines. The protoplasts obtained from various transgenic lines expressing *GFP* were used for analysis including *Nb:GFP*, *Nb:GRX-GFP*, and *Nb:Δ2MGRX-GFP*. **b** Western blot analysis of CcGRXS12-fused GFP and free GFP in the transgenic lines (1. *Nb:GFP*; 2. *Nb: GRX-GFP*; 3. *Nb:Δ2MGRX-GFP*). Visualization was performed for GFP fluorescence, chlorophyll autofluoresence, and nuclear staining with DAPI

lines following viral infection was performed using Coomassie stained gels. At 7 dpi, no difference in viral CP accumulation was found between the inoculated and systemic leaves, or between the transgenic lines under study. Nevertheless, at 14 and 28 dpi, *CcGRXS12* overexpressing lines showed reduced accumulation of viral CP compared to those of control plants, which were transformed with vector devoid of GRX. At 28 dpi, transgenic lines overexpressing *CcGRXS12* showed a significant reduction in viral CP accumulation compared to the GFP expressing lines (Fig. 4a). Northern blot analysis for viral gRNA accumulation showed that no difference was observed between the systemic and inoculated leaves or between different transgenic lines at early stage of infection (7 dpi; Fig. 4b). However, at the late stage of infection (28 dpi), the transcript level of viral gRNA in the *Nb:GFP*-infected plants were relatively high than other *CcGRXS12* overexpressing lines. The relative ratio of viral RNA accumulation in the *Nb:GRX*, *Nb:GRX-GFP* and *Nb:GRX-GFP* was 0.65, 0.05 and 0.11, respectively, when normalized with reference to 1.0 for the *Nb:GFP*-infected lines (Fig. 4b). These results demonstrate that overexpression of *CcGRXS12* does not inhibit virus accumulation at early stage but it severely attenuates the accumulation of viral nucleic acids during the later stages of infection.

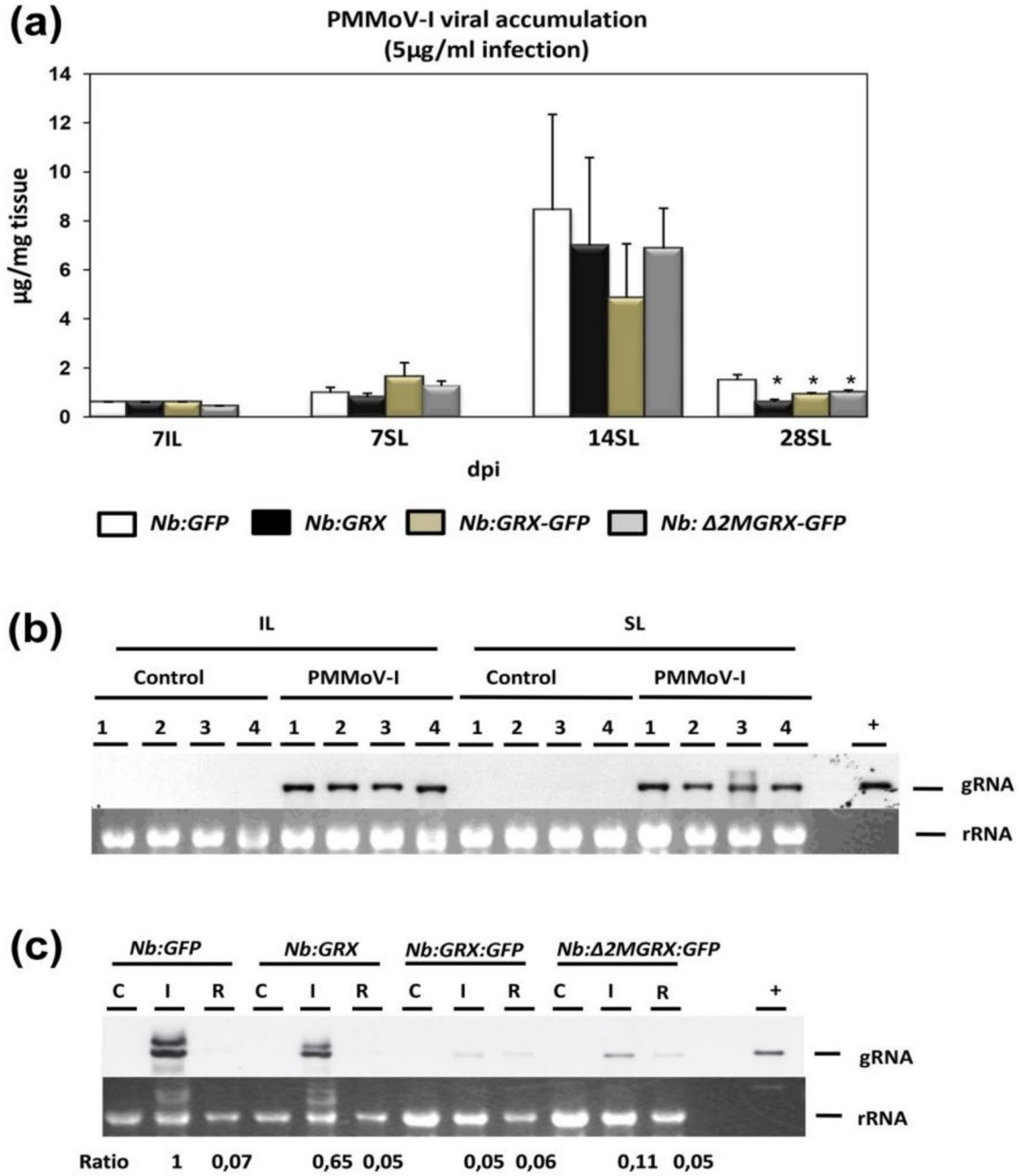

Fig. 4 **a** PMMoV-I coat protein accumulation at different time periods (7, 14, and 28 dpi) in various transgenic lines of *N. benthamiana*. IL—inoculated leaves; SL—systemic leaves. Results were the median of three experiments and were expressed as µg of virus per mg of fresh tissue. Standard deviations are shown as error bars, and significant differences when compared with *Nb:GFP* are indicated by asterisks ($p < 0.05$). Northern blot analysis of viral RNA accumulation at 7 dpi (**b**) and 28 dpi (**c**). The transgenic lines are represented with numbers. In (**b**), 1—*Nb:GFP*; 2—*Nb:GRX*; 3—*Nb:GRX-GFP* and 4—*Nb:Δ2MGRX-GFP*. The samples analyzed at 28 dpi were marked with alphabets. C—mock control; I—infected; R—recovered leaves. Around 50 ng of RNA extracted from PMMoV-I virus was used as positive control (+). Ratio shown at 28 dpi is the ratio of gRNA accumulation with respect to *Nb:GFP* lines. The lower panels of (**b**, **c**) are the ribosomal RNA (rRNA) stained with ethidium bromide that served as the loading control

CcGRXS12 does not inhibit viral RNA replication

In order to study the inhibitory role of *CcGRXS12* towards viral replication, protoplasts obtained from different transgenic lines were infected with viral RNA and the accumulation of the viral CP dynamics was investigated. Viral CP accumulation ascertained through Western blot revealed similar expression in all lines irrespective of *GFP*- or

CcGRXS12-expressing lines (Fig. 5a). Thus, these results suggest that *CcGRXS12* does not inhibit the viral RNA replication.

Expression dynamics of defense genes

To understand the virus resistant mechanism provoked by *CcGRXS12* in plants, the expression of selective transcripts involved in SA pathway (PR-1, PR-5 and PR-2a), JA/ET pathway (PR-2d) (Van Loon et al. 2006), auxin-induced GST marker (pCNT103) (van der Zaal et al. 1987; Droog et al. 1995) were studied during early (7 dpi) and late stages (28 dpi) of viral infection. At 7 dpi, samples were taken from the inoculated and systemic leaves of the infected plants while at 28 dpi, plants recovered from PMMoV-I infection were used. Thus, transcript analysis was performed in both the symptomatic and asymptomatic leaves. PMMoV-I-inoculated leaves from *N. tabacum* cv Xanthi (a well-documented PR protein expressing host) (Stintzi et al. 1993; Van Loon et al. 2006), served as a positive control.

At 7 dpi, high level of SA pathway-related PR transcript accumulation was found in the PMMoV-I-inoculated leaves with no detection in the mock-inoculated leaves, and the level of expression is same irrespective of the transgenic plants (Fig. 6a). Expression of basic PR-2d was found in both the mock- and PMMoV-I-inoculated leaves as the mechanical injury induce JA/ET marker genes. Systemic leaves of the PMMoV-I-infected plants showed low level of expression while no expression in the mock-inoculated control plants.

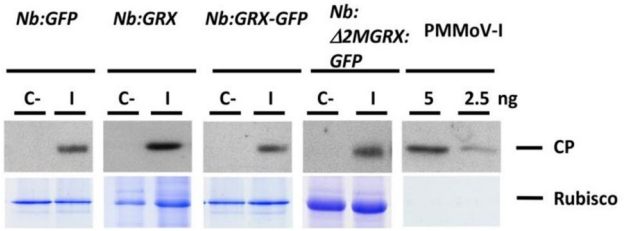

Fig. 5 Detection of PMMoV-I coat protein (CP) by western blot using the protoplasts of various transgenic lines. Purified PMMoV-I (5 and 2.5 ng) was used as positive control. *C* control uninfected protoplast; *I* infected protoplast. Lower panels show Coomassie staining of protein as loading control

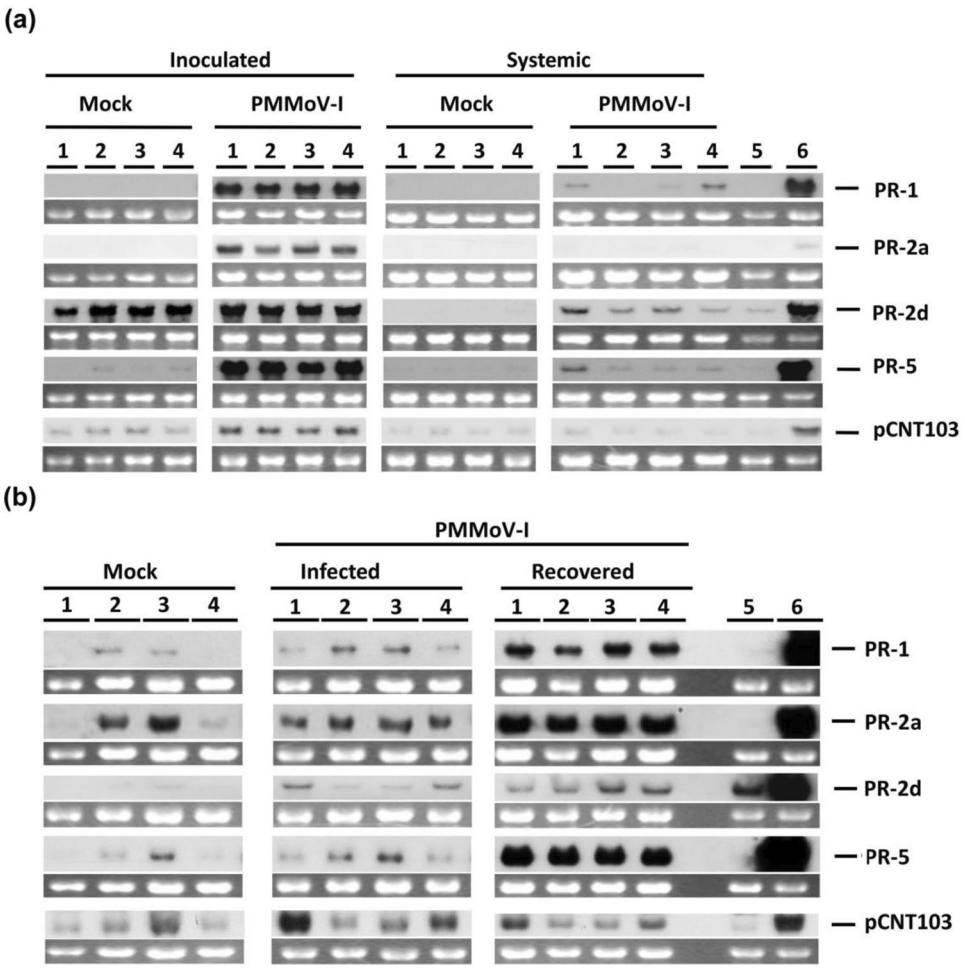

Fig. 6 Northern blot analysis of PR transcripts involved in various hormonal pathways (SA, JA/ET and auxin) from mock and PMMoV-I-infected plants. The expression analysis was performed at 7 dpi (**a**); and 28 dpi (**b**). The different transgenic lines were marked with numbers represent: 1—*Nb:GFP*; —*Nb:GRX*; 3—*Nb:GRX-GFP* and 4—*Nb:Δ2MGRX-GFP*; 5 and 6—mock and PMMoV-I-inoculated leaves from *N. tabacum Xanthi*-nc plants, respectively. The lower panel of each probe shows the ribosomic RNA (rRNA) stained with ethidium bromide. The control (mock) and infected plants were marked on top of the figure

At 28 dpi, in the mock-inoculated plants, the accumulation of SA pathway PR transcripts was found in the *CcGRXS12* (targeted to the chloroplast) overexpressing lines. In the symptomatic leaves of the PMMoV-I-infected plants, high level of SA pathway PR transcripts was accumulated in the *Nb:GRX* and *Nb:GRX-GFP* transgenic lines, whereas the *Nb:GFP* and *Nb:Δ2MGRX-GFP* lines accumulated low levels. The accumulation of JA/ET pathway (PR-2d) and GST (pCNT103) transcripts were found to be suppressed in the *Nb:GRX* and *Nb:GRX-GFP* transgenic lines when compared with the *Nb:GFP* and *Nb:Δ2MGRX-GFP* lines. In the asymptomatic (recovered) leaves of the PMMoV-I-infected plants, the accumulation of SA pathway PR transcripts was found to be very high (two- to three-fold), whereas no significant difference for JA/ET pathway marker transcript was observed when compared with the symptomatic leaves. Between the transgenic lines, no significant differences were found in the accumulation of transcripts from the SA pathway and JA/ET pathway, whereas the GST (pCNT103) marker transcript was reduced in the *CcGRXS12* overexpressing lines when compared to the free *GFP* expressing control line.

Effect of *CcGRXS12* overexpression on redox carrier molecules

At the later stage of PMMoV-I infection (28 dpi), viral suppression and differences in phytohormonal PR transcript accumulation were observed in the plants overexpressing *CcGRXS12*. Redox carrier molecules are known to play significant roles during the pathogen attack and during the induction of defense genes (Pétriacq et al. 2013). Hence, the accumulation of redox carrier molecules (oxidized and reduced forms of PNs) were analyzed in all the transgenic plants at late stage of infection (28 dpi) (see Fig. 7).

In the mock-inoculated (control) plants, the accumulation level of PNs (NAD(P)/(H)) in the free GFP- and *CcGRXS12* overexpressing lines were similar, and no significant difference exist among the transgenic lines. Compared to the mock control plants, the PMMoV-I-infected plants

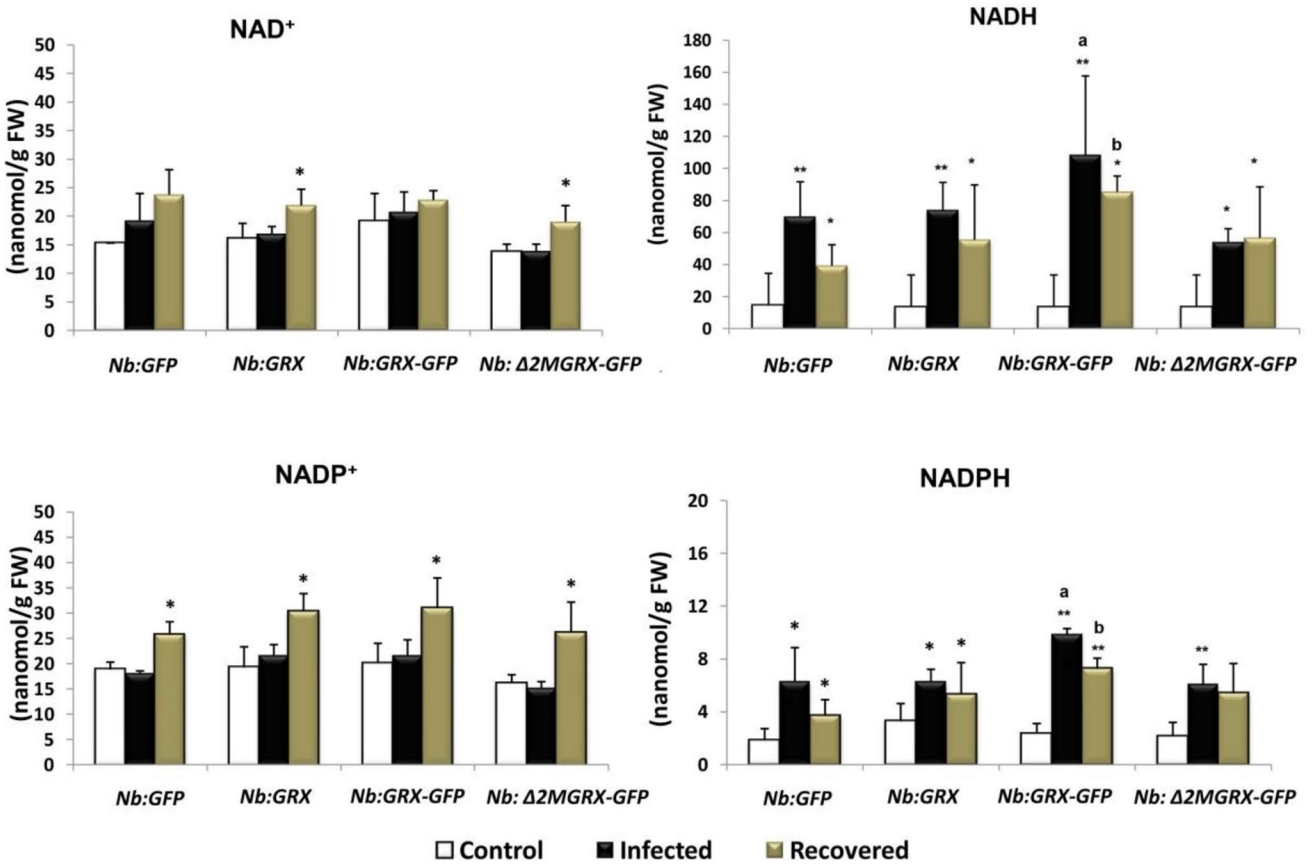

Fig. 7 Analysis of pyridine nucleotides (PN) contents in the control, infected and recovered leaves of various transgenic lines. The levels of NAD^+, $NADP^+$, NADH and NADPH were expressed as nanomoles per gram of fresh tissues (nmol/g FW). The significant difference between the mock-inoculated control and PMMoV-I-infected plants is indicated by asterisks (*) significant difference at ($p < 0.05$), and double (**) significant differences at ($p < 0.001$). Significant differences among the different lines in PMMoV-I-infected plants and recovered plants was noted by the alphabetical letter 'a' and 'b', respectively, at $p < 0.05$

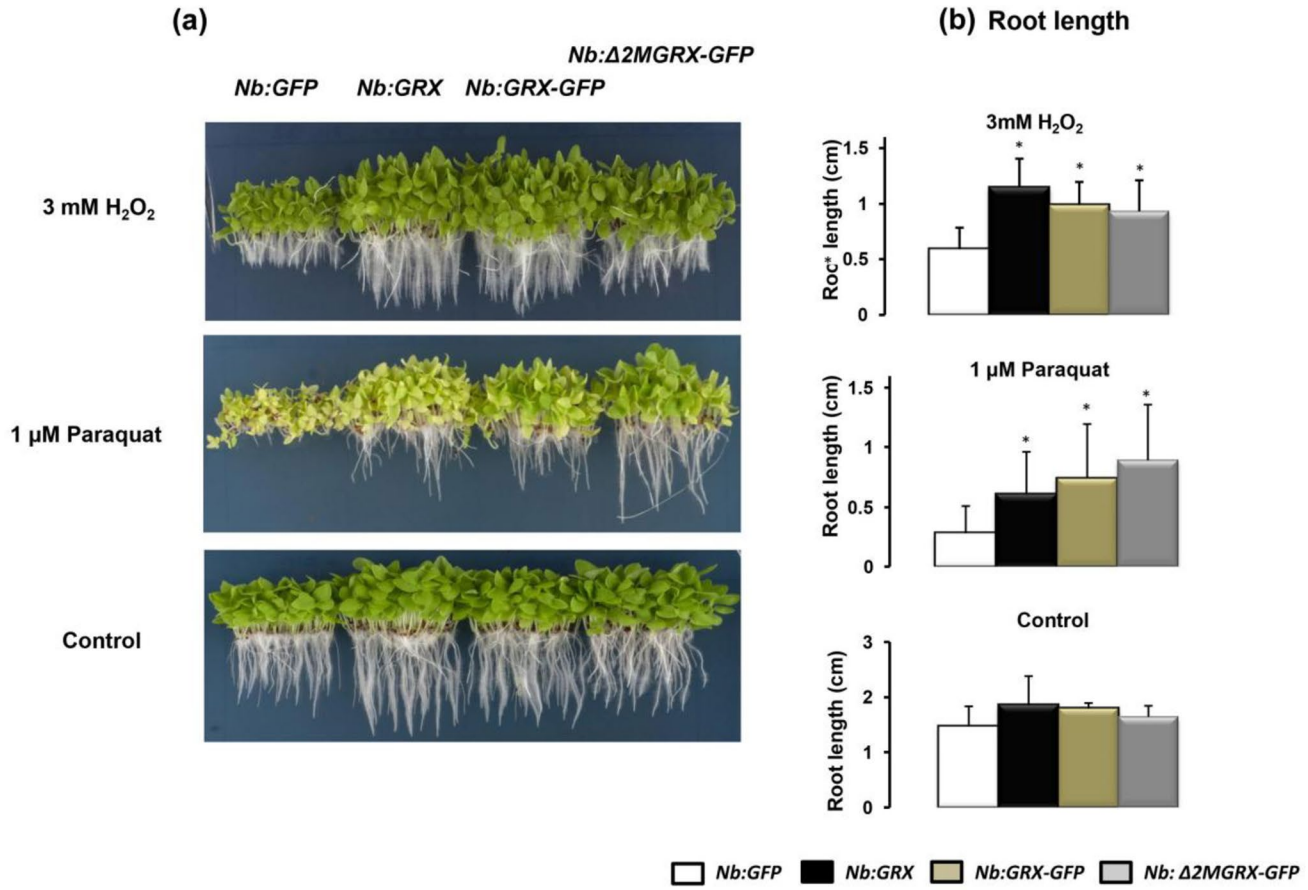

Fig. 8 **a** Phenotype of 12-day-old *N. benthamiana* transgenic lines grown under normal and oxidative stress conditions. b Root length measurement of 30 seedlings for triplicate. The length of the primary roots of seedlings was measured in cm. Significant differences between the *Nb:GFP* and *CcGRXS12* overexpressing lines were represented by asterisks (*) at $p < 0.05$)

(symptomatic leaves) showed high, but non-significant, accumulation of oxidized form of PNs (NAD^+ and $NADP^+$). Asymptomatic leaves showed higher accumulation of (NAD^+ and $NADP^+$), and the accumulation level of $NADP^+$ was significantly higher than the mock control and symptomatic plants.

In the PMMoV-I-infected plants, accumulation of the reduced form of PNs (NADH and NADPH) in the symptomatic and asymptomatic leaves was significantly increased compared to mock control plants. NADH accumulation in the symptomatic leaves was seven- to ninefold higher than the mock control plants. The accumulation level of NADH in the *Nb:GRX-GFP* line was found to be significantly higher when compared with other lines. Although increase in NADH level was observed in the asymptomatic leaves, the accumulation level was lower than the symptomatic leaves of the infected plants. The NAD pool is increased considerably in the infected plants, and it was mainly due to NADH accumulation. Thus, in the PMMoV-I-infected plants, the NAD pool gets shifted considerably towards its reduced form. Increase in NADPH content was found in the PMMoV-I-infected plants (symptomatic and asymptomatic leaves) and symptomatic infected plants showed significantly higher accumulation. As with NADH, the accumulation of NADPH in the infected *Nb:GRX-GFP* plants was significantly higher when compared with other lines. Even though, the level of NADPH was increased in the PMMoV-I-infected plants, the NADP pool was maintained in the oxidized state.

Role of *CcGRXS12* in abiotic stress tolerance

Contribution of *CcGRXS12* to abiotic stress tolerance was studied by root growth assay. When transgenic lines were grown in a media containing 3 mM H_2O_2 or 1 µM paraquat, plants overexpressing *CcGRXS12* and its derivatives showed significantly increased primary root elongation than the free *GFP* transgenic line ($P < 0.05$). The effect of paraquat treatment was stronger than the H_2O_2. The abiotic stress tolerance observed was independent of protein localization as *Nb:Δ2MGRX-GFP* transgenic lines also show better growth in the oxidative media. No significant differences shown between the free *GFP* and *CcGRXS12* overexpressing plants when grown in the control media. Thus, overexpression of

CcGRXS12 in plants increased the abiotic stress tolerance caused by either H_2O_2 or paraquat.

Functional substitution of *CcGRXS12* in yeast *Δgrx5* mutants

In yeast, *ScGRX5* was characterized to carry out the Fe–S cluster assembly mechanism (Rodrıguez-Manzaneque et al. 2002). The role of plant GRX in Fe–S cluster assembly mechanism was studied through yeast *Δgrx5* complementation studies (Bandyopadhyay et al. 2009). To examine whether *CcGRXS12* substituted the function role of *ScGRX5* in yeast, yeast *Δgrx5* mutants were transformed with *CcGRXS12*. The results revealed that *CcGRXS12* could not rescue the *Δgrx5* mutants in the growth defective media (Fig. 8a) and the media containing external oxidants (Fig. 8b). Further, high level accumulation of free iron (Fig. 8c) and low relative aconitase to MDH ratio (Fig. 8c, d) in the *Δgrx5* mutants were not restored to normal level when *CcGRXS12* was transformed. These results suggest that *CcGRXS12* could not perform the function for Fe–S cluster assembly in yeast *Δgrx5* mutants.

Discussion

The current study observed an increase in transcript accumulation of a chloroplastic class I GRX gene from the S12 subgroup (*CcGRXS12*) in *Capsicum chinense* plants infected with compatible (PMMoV-I) and incompatible (PMMoV-S) plant viruses. The elevated levels of *CcGRXS12* during viral infection and cold treatment suggest its potential role in vital processes under both viral infection and abiotic stress conditions. Previous studies, based on the thermodynamic properties of PtGRXS12 proteins, have suggested that this protein tends to accumulate during GSH-mediated mild oxidative stress conditions in plants and during the glutathionylation process in Arabidopsis (Courturier et al. 2009a; Dixon et al. 2005; Zaffagnini et al. 2012). The PMMoV-I infection and cold treatment induce oxidative stress conditions in plants, leading to a disturbance in the GSH redox status within cells (Hakmaoui et al. 2012; Kumar et al. 2016). The observed differential expression of *CcGRXS12* transcripts during PMMoV-I infection and cold stress conditions in Capsicum plants may be attributed to its role in GSH-mediated oxidative stress.

The CSYS active site of GRX (GRXS12) has been reported in yeast, plants and insect but none from prokaryotes and primitive photosynthetic organisms (*Chlamydomonas reinhardtii*) were reported to date, suggesting its definite functions in the higher organisms. In vitro oxidoreductase activity testing for CcGRXS12 revealed its capability to reduce GSH-disulfides formed in the HED assay, similar to poplar PtGRXS12 (Couturier et al. 2009b). However, the catalytic efficiency of CcGRXS12 was found to be tenfold less efficient than PtGRXS12 (Fig. 1B). The deglutathionylation property exhibited by GRXS12 proteins is crucial for regenerating antioxidant enzymes such as MSRB1 (Vieira Dos Santos et al. 2007) and PrxII protein (Gama et al. 2008), contributing to the maintenance of redox balance in plant cells. In the chloroplasts of plant cells, both class I GRX (C5/S12) and class II GRXs (S14–S17) coexist. Class I GRXs reduce substrates by utilizing reducing equivalents from GSH, while class II GRX (GRXS14) uses reducing equivalents from FTR. Thus, the presence of the GRXS12 protein serves multiple functions in the plant system, particularly where GSH plays a pivotal role.

CcGRXS12 role in hormonal pathway activation

As GRXs are abundant in the plant genome, the functional role of the isolated gene was studied with regards to plant–pathogen interaction by overexpressing it in *N. benthamiana* Domin plants. Members of the TRX family protein (NtTRXh3) were reported to reduce the multiplication and pathogenicity of TMV and CMV in tobacco plants which was accompanied with the activation of SAR defense-related PR genes (Sun et al. 2010). In order to comprehend, if *CcGRXS12* has any molecular role in the activation of systemic acquired resistance (SAR) mechanism, SA-, JA/ET-, and auxin-induced GST transcripts, were analyzed in the transgenic plants under study. The *CcGRXS12* overexpressing lines did not show difference in PR transcript when compared with *GFP* expressing plants at the early stage of plant growth or infection (i.e., 7 dpi). However, at 28 dpi, high levels of SA pathway PR transcripts were accumulated in the mock (control) lines of *CcGRXS12*, targeted to chloroplast (*Nb:GRX* and *Nb:GRX-GFP* lines) (Fig. 6b). Although higher accumulation of PR proteins was reported during the senescence stage (Obregón et al. 2001) in tobacco plants, the increased accumulation of SA-regulated PR proteins observed in the *CcGRXS12* transgenic plants appears to be related with the expression of *CcGRXS12* targeted to chloroplast. Moreover, mRNA accumulation corresponding to PR was not detected in the *N. benthamiana* plants expressing free *GFP* at that stage of development. Further the analysis of the defense marker transcripts showed that the overexpression of *CcGRXS12* in chloroplast (*Nb:GRX* and *Nb:GRX-GFP* lines) suppress the JA/ET and GST transcript in the PMMoV-I-infected lines. Previous reports have shown that the activation of SA pathway suppresses the JA-responsive genes through the induction of GRXs which interacts with the transcription factors involved in the SA-JA antagonism mechanism (Zander et al. 2012; Wasternack and Hause 2013). Salicylic acid pathway inhibits the auxin response pathway by universally suppressing the

auxin-related genes and auxin receptor genes (Wang et al. 2007; Kong et al. 2020). The results described herein were in accordance with those observed for *Arabidopsis* GRX480, that when ectopically expressed in *Arabidopsis* enhanced the expression of SA-inducible marker genes while inhibited the expression of JA-regulated genes (Nadamukong et al. 2007). Viral accumulation was inhibited in the truncated GRX (*Nb:Δ2MGRX-GFP*) lines, but the SA pathway activation and suppression of JA/ET pathway in the infected lines were not observed in these lines. This shows that apart from SAR activation, *CcGRXS12* could use other unknown mechanism for viral inhibition. Activation of SA pathway-related transcripts in the mock control plants; and SA-mediated JA/ET antagonism mechanism found in the infected lines of *Nb:GRX* and *Nb:GRX-GFP* show that the presence of *CcGRXS12* in the chloroplast is necessary for mediating this process as it was not observed in the truncated form of the *CcGRXS12*-expressing line (*Nb:Δ2MGRX-GFP*) and free *GFP* expressing line (*Nb:GFP*). Possibly, *CcGRXS12* may activate the SA pathway genes either by (i) promoting the SA biosynthesis inside the chloroplast (or) (ii) affect the redox status of proteins (or) transcription factors involved in the transcription of SA pathway genes thereby mediating the SA-/JA/ET antagonism in virus-infected plants. GRXs were reported to synthesis phytohormones inside the plants. In rice, overexpression of the *OsGRX6* increased the cytokinin and gibberellic acid levels (El-Kereamy et al. 2015; Sharma et al. 2013) by activating the phytohormonal pathway synthesizing genes. In *Arabidopsis*, the activity of GCL, a key enzyme involved in the SA biosynthesis in chloroplast is affected by the redox-dependent post-translational modification (Hothorn et al. 2006; Hicks et al. 2007). Hence, it is of future interest to study whether *GRXS12* contribute to SA biosynthesis within the chloroplast by modifying the SA biosynthetic pathway genes.

Overexpression of *CcGRXS12* inhibits viral accumulation

When the transgenic plants were infected with PMMoV-I, no difference in viral disease symptom was observed at early stage of infection among the *GFP* and *CcGRXS12* overexpressing lines. However, recovery of the plants was more obvious in the *CcGRXS12* overexpressing lines at later stages of infection (28 dpi). At early stage of infection (7 dpi), no difference in the level of virus accumulation between the *CcGRXS12* overexpressing lines and the free *GFP* expressing line, while at the late stage of infection, overexpression of *CcGRXS12* inhibited the viral accumulation when compared to the transgenic *GFP* control (Fig. 4a–c). Reduced accumulation of virus in the *Nb:GRX-GFP* expressing line showed that the effect was dose dependent as *CcGRXS12* expression was found to be 10 times higher in this transgenic line (Fig. 4c). The viral suppression was independent of *CcGRXS12* localization, as *CcGRXS12* targeted to the cytoplasm also inhibited viral accumulation similar to the lines wherein *CcGRXS12* was targeted to chloroplast. Protoplast infection studies showed that *CcGRXS12* and its derivative expressions are not inhibiting the viral replication. This result was different from the previous reports of Auwerx et al. (2009), where it was shown that the replication of HIV was inhibited by the expression of glutaredoxin-1 in the mammalian cell system. Montes-Casado et al. (2010) have shown that the reduction of PMMoV-I virus accumulation was due to a lower number of infected cells in the systemic leaves of the *CcGRXS12* transgenic plants. Hakmaoui et al. (2012) have shown that tobacco plants infected with PMMoV-I virus recovered at late stage (28 dpi) of infection by upregulating the expression of superoxide dismutase and maintaining the adequate level of peroxiredoxins which are the key antioxidants of the cell. Increased ROS accumulation and decline in antioxidants are prerequisite for the establishment and spread of virus (Clarke et al. 2002; Hakmaoui et al. 2012). During virus invasion, plants use antioxidant machinery to bring down the oxidative stress condition under control. Virus invasion induced the expression of Glutathione-S-Transferase (GST) to control the oxidative stress condition (Chen et al. 2013; Xu et al. 2013; Pavan Kumar et al. 2017; Skopelitou et al. 2012). At 28 dpi, the expression of auxin-induced glutathione-S-transferase (GST) (pCNT103) was lowered in the infected and recovered leaves C*cGRXS12* and its derivatives expressing line while in the free *GFP* expressing lines it was at high level. The reduced accumulation of pCNT103 transcripts in the symptomatic and asymptomatic leaves of *CcGRXS12*-expressing lines showed that the protein (CcGRXS12) enhances ROS-scavenging activity in the *CcGRXS12* overexpressing line, and thus limit the virus induced oxidative stress condition. It is important to mention that *AtGRXS12* could regenerate PrxII and MSR B antioxidants in *Arabidopsis* (Vieira Dos Santos et al. 2007; Gama et al. 2008). Individual GRXs have different regulatory roles on ROS homeostasis. Overexpression of *ROXY1* GRX accumulate higher ROS content, whereas *ROXY18/GRXS13* overexpression reduces the ROS accumulation (Wang et al. 2009; La Camera et al. 2011). In the present study, in vitro abiotic stress tolerance assays showed that *CcGRXS12* overexpressing lines were found to be resistant against oxidative stress conditions, caused by paraquat and H_2O_2. Overall, the results indicated that the protein could able to protect the plants from oxidative stress condition at the time of pathogen attack.

CcGRXS12 maintains the redox status of the plant cells

Redox status of the cell is sensed and signaled inside the cells by the redox carrier molecules (Ascorbate, Glutathione

and Pyridine nucleotides) in oxidized and reduced forms. The inter-conversion of the redox carrier molecules between the reduced or oxidized forms as ascorbate (ASC, DHA), glutathione (GSH, GSSG) and pyridine nucleotides (NAD(P)+, NAD(P)H) depends on the cellular redox environment of the cell. *N. benthamiana* plants infected with PMMoV-I virus, shift the redox carrier molecules (ASC, DHA; GSH, GSSG) more towards oxidized condition (Hakamoui et al. 2012). In our work, we have found that PMMoV-I infection of *N. benthamiana* transgenic lines increased the PNs level by shifting PN towards reduced condition as the levels of NADH and NADPH were found to be significantly higher in the PMMoV-I-infected plants than in the mock-inoculated control plants at 28 dpi (Fig. 9). Increase in PN contents improve tolerance to oxidative stresses, which was caused by biotic and abiotic stresses (Dutilleul et al. 2005; Pétriacq et al. 2012; Ogawa et al. 2016; Awasthi et al. 2019; Zhao et al. 2019). Among the PNs analyzed, increase in NADH level showed four- to eightfold in the PMMoV-I-infected plants which indicated that NADH is a good marker for PMMoV-I infection. Several previous studies also imply that increases in NADH content is a mandatory process during biotic and abiotic stress-related defense mechanisms (Ishikawa et al. 2009; Pétriacq et al. 2016, 2012; Ogawa et al. 2016).

Noctor, (2006) has proposed that reduced form of PNs produced in the cells are utilized by the NAD(P)H consuming enzymes which are involved in the synthesis of ROS and RNS in the cell which may act as a signaling molecule for the plant defense mechanism. Increase in NADH content in the PMMoV-I-infected and recovered plant leaves produces an imbalance in the NADH/NAD^+

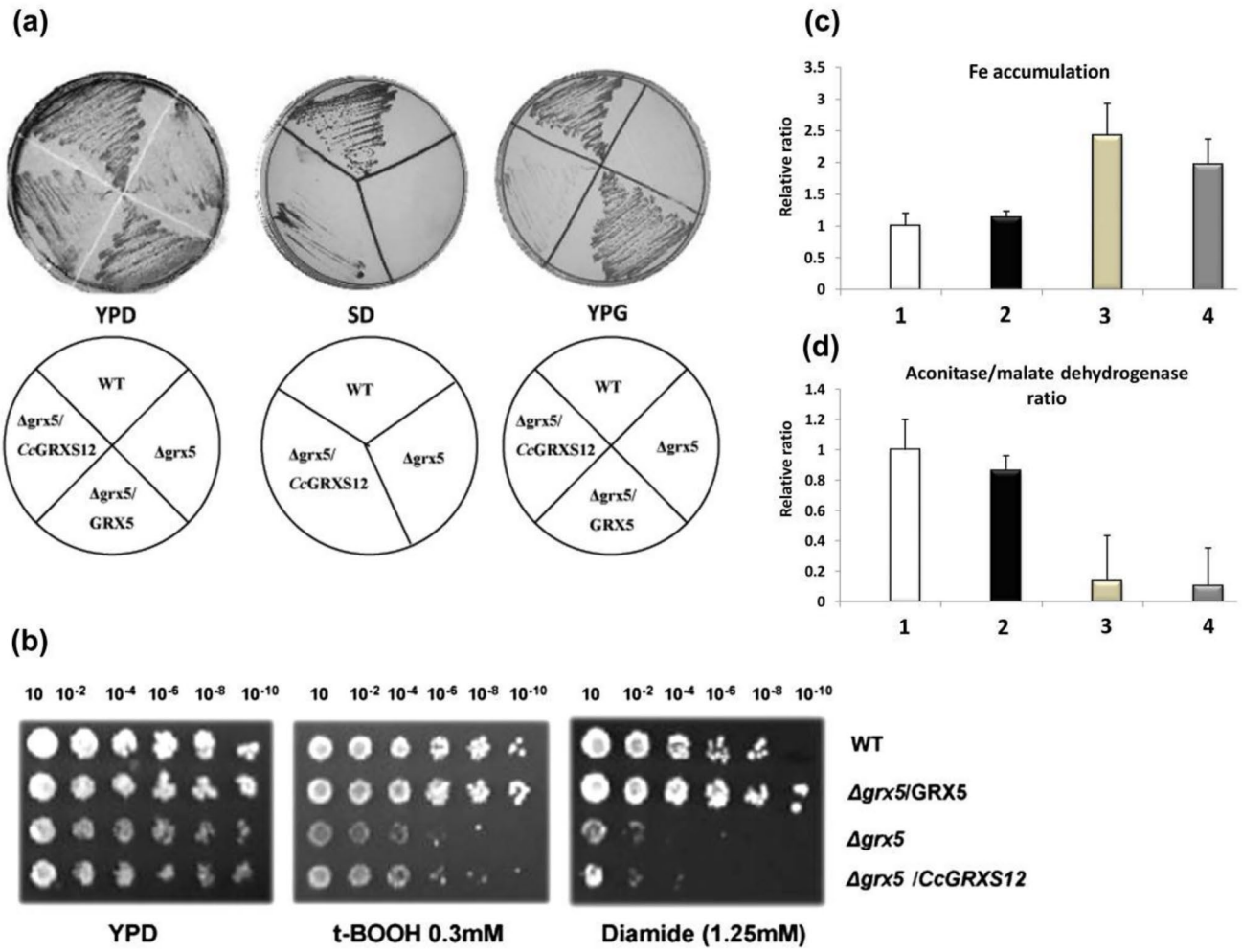

Fig. 9 *CcGRXS12* complementation assay in yeast Δ*grx5* mutants. **a** Analysis of the rescue effect of *CcGRXS12* in defective media. The different yeast strains (WT—wild type; Δ*grx5*; Δ*grx5/GRX5*; Δ*grx5/CcGRXS12*) were grown in the glucose (YPD), minimal (SD) and Glycerol (YPG) media for 3 days at 30 °C. **b** Sensitivity towards oxidants were analyzed by grown over YPD media containing t-BOOH and diamide for 3 days at 30 °C. **c** Relative accumulation of free iron in the different yeast strains. **d** Relative ratio of aconitase to malate dehydrogenase in different yeast strains. In c and d, 1, 2, 3, and 4 represent yeast strains such as wild type, Δ*grx5*, Δ*grx5/GRX5* and Δ*grx5/CcGRXS12*, respectively

that triggers the production of ROS (Millar et al. 2001) or the regulation of cellular antioxidant systems (Dutilleul et al. 2003). Ogawa et al. (2016) have shown that Arabidopsis KO-*nudx6/7* mutants which accumulate high level of NADH are accompanied with increased biotic and abiotic stress tolerance. Increase in NADH in these mutant lines brings biotic/abiotic stress tolerance through the expression of biotic and abiotic stress responsive genes. The genes positively correlated with the increased NADH level belongs to SA pathway (PR1, PR5), JA/ET pathway genes (PDF1.2), oxidoreductase and post-translational modifying (PTM) enzymes. The genes activated by the increased NADH content differed from H_2O_2 pathway-mediated gene expressions. In our work, we found that within the infected transgenic lines, only *Nb:GRX-GFP* line showed significantly higher NADH and NADPH accumulation at 28 dpi which was accompanied with enhanced virus resistance, which demonstrated that high level *CcGRXS12* expression respond to pathogen infection with increased NADH content.

Redox carrier molecules versus PR proteins

Previous studies have correlated the phenomenon of PN accumulation and PR gene expression. For example, extracellular application of PN induce plant resistance to pathogen (Zhang and Mou 2009; Alferez et al. 2018; Wang et al. 2016; Sidiq et al. 2021). Reducing the level of PN through genetic manipulation compromise the activation of SA pathway and pathogen resistance (Li et al. 2021). Nevertheless, the present study has proven that *CcGRXS12*-mediated PR transcript accumulation is independent of PN accumulation as it was found that PN accumulation in the different transgenic plants and the mock-inoculated control plants are comparable but the accumulation of SA pathway transcript was high in *Nb:GRX-GFP* line (Fig. 6b). Further at 28 dpi, PN accumulation in the asymptomatic leaves was found to be lower than their infected counterparts, which is contrast with PR accumulation. Thus, *CcGRXS12*-mediated PR gene expression was independent of PN levels under pathogenic and non-pathogenic conditions.

CcGRXS12 in abiotic stress tolerance

It has been demonstrated that many plant GRX proteins protect the plants from oxidative stress conditions created during abiotic stress conditions (Wu et al. 2012, 2017). Treatment of plants with paraquat generates ROS in chloroplasts due to auto-oxidation of paraquat radicals generated by electrons from the reaction center of PSI (Taiz and Zeiger 2010; Krieger-Liszkay et al. 2015), thereby inducing oxidative damage. *CcGRXS12* overexpression enhances the plants tolerance against oxidative stress conditions caused by H_2O_2 and paraquat irrespective of the protein localization. Different mechanisms for GRX-mediated ROS-scavenging were proposed; GRXs detoxify ROS toxicity through lowering the accumulation of superoxide ion radicals (Laporte et al. 2012; Ning et al. 2018) or by regenerating the antioxidant proteins (Rouhier et al. 2007; Wu et al. 2012; Guo et al. 2010; Sharma et al. 2013; Morita et al. 2015). Apart from this, GRXs were reported to scavenge ROS through interaction with transcription factors involved in the stress-related genes expression (Hu et al. 2015; Wu et al. 2012) or by protecting the thiol groups on the enzymes (Morita et al. 2015). The mechanisms through which *CcGRXS12* induce abiotic stress tolerance in *N. benthamiana* have not been analyzed in this work; however, it is plausible that the overexpression of *CcGRXS12* could activate the expression of genes involved in the antioxidant mechanisms either in the cytoplasm or the chloroplast. Previously, in vitro studies have reported that *AtGRXS12* could able to regenerate PrxII and MSR B which are the major antioxidants in plant system (Vieira Dos Santos et al. 2007; Gama et al. 2008).

CcGRXS12 in Fe–S cluster assembly mechanism

Fe–S cluster containing proteins were found to be abundant in the chloroplast, mitochondria and throughout the cell (Przybyla-Toscano et al. 2018). Involvement of GRX5 protein in Fe–S cluster assembly was first studied in yeast where the deletion of *GRX5* caused deficient in the synthesis of Fe–S cluster containing proteins and further leads to the accumulation of iron which increases the sensitivity of yeast cells towards oxidative stress conditions (Rodriguez-Manzaneque et al. 1999, 2002). Many plant *GRX*s substitute the function of *GRX5* in yeast (Cheng et al. 2006; Cheng 2008; Bandyopadhyay et al. 2008). In the current study, the overexpression of *CcGRXS12* in yeast *Δgrx5* mutant could neither restore the Fe–S enzyme activities nor suppress iron accumulation (Fig. 8C, D). Thus, *CcGRXS12* could not participate in Fe–S cluster assembly in yeast but in plants, it is still uncertain. The structural analysis of populous PtGRXS12 the closest paralog of CcGRXS12 found that the presence of Trp at -1 position prevents the protein from Fe–S cluster assembly (Couturier et al. 2009b). However, the later studies on AtGRXC5 structure observed that amino acids at other sites are the deciding factors for the Fe–S cluster assembly mechanism apart from Trp at -1 position (Couturier et al. 2011). Thus, yeast transformation studies indicated that the protein may not participate in the biogenesis of Fe–S cluster assembly or in the regulation of iron homeostasis in the chloroplasts.

In conclusion, overexpression of *CcGRXS12* in *N. benthamiana* protects the plants from the oxidative stress conditions created during the biotic and abiotic stresses. CcGRXS12 protein possesses oxidoreductase activity as it could reduce the disulfide bonds formed between GSH and

substrate during the HED assay but not able to participate in Fe–S cluster assembly mechanism. The involvement of this protein in multiple stresses warrants further investigation so that it could be exploited for engineering crops with improved stress tolerance.

Availability of sequence information

The gene (*CcGRXS12*) sequence used in this work was deposited in the NCBI GenBank site with the accession number: BankIt2748931 CcGRXS12 OR611922.

Acknowledgements Our sincere thanks to Dr. Maria Terresa Serra Yoldi, who was the doctoral mentor for R.M. Saravana Kumar and also provided the space for conducting doctoral research studies. The authors thank Dr. Isabel Garcia Luque for her support and knowledge during the research studies. We thank Dr. Enrique Herrero for providing the yeast strains and helps to carry out yeast transformation studies. I thank Dr. Victoriana Palpuestra for helping me to analyze pyridine nucleotide.

Author contributions RMSK designed the research, performed the experiments, interpreted the results, and wrote the manuscript. SVR assisted in the preparation of the manuscript and offered critical comments. ZS, ST, NPCN and AKB assisted to interpret the results and edited the manuscript. SK and RS did the revision and final editing of the manuscript. All the authors have read and approved the final version of the manuscript.

Funding This work was supported by CSIC-JAE program during R.M. Saravana Kumar pre-doctoral studies.

Data availability All data generated or analysed during this study are included in this published article.

Declarations

Conflict of interest None.

References

Akbar S, Wei Y, Yuan Y, Khan MT, Qin L, Powel CA, Chen B, Zhang M (2020) Gene expression profiling of reactive oxygen species (ROS) and antioxidant defense system following Sugarcane mosaic virus (SCMV) infection. BMC Plant Biol 20:532

Alferez FM, Gerberich KM, Li JL, Zhang Y, Graham JH, Mou Z (2018) Exogenous Nicotinamide Adenine Dinucleotide induces resistance to citrus canker in citrus. Front Plant Sci 9:1472

Alonso E, Garcia-Luque I, de la Cruz A, Wicke B, Avila-Rincon MJ, Serra MT, Castresana C, Diaz-Ruiz JR (1991) Nucleotide sequence of the genomic RNA of pepper mild mottle virus, a resistance-breaking tobamovirus in pepper. J Gen Virol 72:2875–2884

Auwerx J, Isacsson O, Söderlund J, Balzarini J, Johansson M, Lundberg M (2009) Human glutaredoxin-1 catalyzes the reduction of HIV-1 gp120 and CD4 disulfides and its inhibition reduces HIV-1 replication. Int J Biochem Cell Biol 41:1269–1275

Awasthi JP, Saha B, Panigrahi J, Yanase E, koyama H, Panda SK (2019) Redox balance, metabolic fingerprint and physiological characterization in contrasting North East Indian rice for Aluminum stress tolerance. Sci Rep 9:8681

Balint-Kurti P (2019) The plant hypersensitive response: concepts, control and consequences. Mol Plant Pathol 20:1163–1178

Bandyopadhyay S, Gama F, Molina-Navarro MM, Gualberto JM, Claxton R, Naik SG, Huynh BH, Herrero E, Jacquot JP, Johnson MK, Rouhier N (2009) Chloroplast monothiol glutaredoxins as scaffold proteins for the assembly and delivery of [2Fe-2S] clusters. EMBO J 27:1122–1133

Bozbuga R, Arpaci BB, Uluisik S, Guler PG, Yildiz HN, Ates SY (2022) Genetic modification of plant hormones induced by parasitic nematodes, virus, viroid, bacteria, and phytoplasma in plant growing. In: Hano C (ed) Plant hormones—recent advances, new perspectives and applications. IntechOpen, Berlin. https://doi.org/10.5772/intechopen.102721

Chen IH, Chiu MH, Cheng SF, Hsu YH, Tsai CH (2013) The glutathione transferase of *Nicotiana benthamiana* NbGSTU4 plays a role in regulating the early replication of bamboo mosaic virus. New Phytol 199:749–757

Chenchik A, Zhu YY, Diatchenko L, Li R, Hill J, Siebert PD (1998) Gene cloning and analysis by RT-PCR. In: Siebert P, Larrick J, Natick MA (eds) BioTechniques books. Science Open Publishers, pp 305–319

Cheng NH (2008) AtGRX4, an Arabidopsis chloroplastic monothiol glutaredoxin, is able to suppress yeast grx5 mutant phenotypes and respond to oxidative stress. FEBS Lett 582:848–854

Cheng NH, Liu JZ, BrockA NRS, Hirschi KD (2006) AtGRXcp, an Arabidopsis chloroplastic glutaredoxin, is critical for protection against protein oxidative damage. J Biol Chem 281:26280–26288

Chomczynski P, Sacchi N (1987) Single-step method of RNA isolation by acid guanidinium thiocyanate-phenol-chloroform extraction. Anal Biochem 162:156–159

Clarke SF, Guy P, Burritt DJ, Jameson PE (2002) Changes in the activities of antioxidant enzymes in response to virus infection and hormone treatment. Physiol Plant 114:157–164

Couturier J, Jacquot JP, Rouhier N (2009a) Evolution and diversity of glutaredoxins in photosynthetic organisms. Cell Mol Life Sci 66:2539–2557

Couturier J, Didierjean C, Jacquot JP, Rouhier N (2010) Engineered mutated glutaredoxins mimicking peculiar plant classIII glutaredoxins bind iron-sulfur centers and possess reductase activity. Biochem Biophys Res Commun 403:435–441

Couturier J, Stroher E, Albetel AN, Roret T, Muthuramalingam M, Tarrago L, Seidel T, Tsan P, Jacquot JP, Johnson MK, Dietz KJ, Didierjean C, Rouhier N (2011) Arabidopsis chloroplastic glutaredoxin C5 as a model to explore the molecular determinants for iron-sulfur cluster binding into glutaredoxins. J Biol Chem 286:27515–27527

CouturierJ KCS, Zaffagnini M, Winger AM, Gualberto JM, Corbier C, Decottignies P, Jacquot JP, Lemaire SD, Didierjean C, Rouhier N (2009b) Structure–function relationship of the chloroplastic glutaredoxin S12 with an atypical WCSYS active site. Jbiol Chem 284:9299–9310

Després C, DeLong C, Glaze S, Liu E, Fobert PR (2000) The Arabidopsis NPR1/NIM1 protein enhances the DNA binding activity of a subgroup of the TGA family of bZIP transcription factors. Plant Cell 12:279–290

Dixon J, Durrheim K, Tredoux C (2005) Beyond the optimal contact strategy: a reality check for the contact hypothesis. Am Psychol 60:697–711

Droog F, Hooykaas P, Van Der Zaal BJ (1995) 2,4-Dichlorophenoxyacetic acid and related chlorinated compounds inhibit two auxin-regulated Type-III tobacco Glutathione S-Transferases. Plant Physiol 107:1139–1146

Dutilleul C, Driscoll S, Cornic G, De Paepe R, Foyer CH, Noctor G (2003) Tobacco leaves require functional mitochondrial

complex I for optimal photosynthetic performance in photorespiratory conditions and during transients. Plant Physiol 131:264–275

Dutilleul C, Lelarge C, Prioul JL, De Paepe R, Foyer CH, Noctor G (2005) Mitochondria-driven changes in leaf NAD status exert a crucial influence in the control of nitrate assimilation and the integration of carbon and nitrogen metabolism. Plant Physiol 139:64–78

Ehrary A, Rosas M, Carpinelli S, Davalos O, Cowling C, Fernandez F, Escobar M (2020) Glutaredoxin AtGRXS8 represses transcriptional and developmental responses to nitrate in *Arabidopsis thaliana* roots. Plant Direct 4:e00227

El-Kereamy A, Bi YM, Mahmood K, Ranathunge K, Yaish MW, Nambara E, Rothstein SJ (2015) Overexpression of the CC-type glutaredoxin, OsGRX6 affects hormone and nitrogen status in rice plants. Front Plant Sci 6:934

Emanuelsson O, Nielsen H, von Heijne G (1999) ChloroP, a neural network-based method for predicting chloroplast transit peptides and their cleavage sites. Protein Sci 8:978–984

Fish WW (1988) Rapid colorimetric micromethod for the quantitation of complexed iron in biological samples. Methods Enzymol 158:357–364

Fodor J, Gullner G, Adam AL, Barna B, Komives T, Kiraly Z (1997) Local and systemic responses of antioxidants to tobacco mosaic virus infection and to salicylic acid in tobacco (Role in Systemic Acquired Resistance). Plant Physiol 114:1443–1451

Gama F, Bréhélin C, Gelhaye E, Meyer Y, Jacquot JP, Rey P et al (2008) Functional analysis and expression characteristics of chloroplastic Prx IIE. Plant Physiol 133:599–610

Garcia-Luque I, Serra MT, Alonso E, Wicke B, Ferrero ML, Diaz-Ruiz JR (1990) Characterization of a Spanish strain of pepper mild mottle virus (PMMV-S) and its relationship to other Tobamoviruses. J Phytopathol 129:1–8

Gibon Y, Blaesing OE, Hannemann J, Carillo P, Höhne M, Hendriks JHM (2004) A robot-based platform to measure multiple enzyme activities in Arabidopsis using a set of cycling assays: comparison of changes of enzyme activities and transcript levels during diurnal cycles and in prolonged darkness. Plant Cell 16:3304–3325

Gilardi P, García-Luque I, Serra MT (1998) Pepper mild mottle virus coat protein alone can elicit the Capsicum spp. L3 gene-mediated resistance. Mol Plant Microbe Interact 11:1253–1257

GuoY HC, Xie Y, Song F, Zhou X (2010) A tomato glutaredoxin gene SlGRX1 regulates plant responses to oxidative, drought and salt stresses. Planta 232:1499–1509

Gutsche N, Holtmannspötter M, Maß L, O'Donoghue M, Busch A, Lauri A, Schubert V, Zachgo S (2017) Conserved redox-dependent DNA binding of ROXY glutaredoxins with TGA transcription factors. Plant Direct 1:e00030

Hajirezaei M-R, Peisker M, Tschiersch H, Palatnik JF, Valle EM, Carrillo N, Sonnewald U (2002) Small changes in the activity of choroplastic NADP+-dependent ferredoxin oxidoreductase lead to impaired plant growth and restrict photosynthetic activity of transgenic tobacco plants. Plant J 29:281–293

Hakmaoui A, Pérez-Bueno ML, García-Fontana B, Camejo D, Jiménez A, Sevilla F, Barón M (2012) Analysis of the antioxidant response of *Nicotiana benthamiana* to infection with two strains of Pepper mild mottle virus. J Exp Bot 63:5487–5496

Herrera-Vásquez A, Carvallo L, Blanco F, Tobar M, Villarroel-Candia E, Vicente-Carbajosa J, Salinas P, Holuigue L (2015) Transcriptional control of Glutaredoxin GRXC9 expression by a salicylic acid-dependent and NPR1-independent pathway in Arabidopsis. Plant Mol Biol Rep 33:624–637

Hicks LM, Cahoon RE, Bonner ER, Rivard RS, Sheffield J, Jez JM (2007) Thiol-based regulation of redox-active glutamate-cysteine ligase from *Arabidopsis thaliana*. Plant Cell 19:2653–2661

Holmgren A, Aslund F (1995) "Glutaredoxin." Methods Enzymol 252:283–292

Hothorn M, Wachter A, Gromes R, Stuwe T, Rausch T, Scheffzek K (2006) Structural basis for the redox control of plant glutamate cysteine ligase. J Biol Chem 281:27557–27565

Hou J, Sun Q, Li J, Ahammed GJ, Yu J, Fang H et al (2019) Glutaredoxin S25 and its interacting TGACG motif-binding factor TGA2 mediate brassinosteroid-induced chlorothalonil metabolism in tomato plants. Environ Pollut 255:113256

Hu Y, Wu Q, Sprague SA, Park J, Oh M, Rajashekar CB, Koiwa H, Nakata PA, Cheng N, Hirschi KD, White FF, Park S (2015) Tomato expressing Arabidopsis glutaredoxin gene AtGRXS17 confers tolerance to chilling stress via modulating cold responsive components. Hort Res 2:15051

Ishikawa K, Ogawa T, Hirosue E, Nakayama Y, Harada K, Fukusaki E, Yoshimura K, Shigeoka S (2009) Modulation of the poly(ADP-ribosyl)ation reaction via the Arabidopsis ADP-ribose/NADH pyrophosphohydrolase, AtNUDX7, is involved in the response to oxidative stress. Plant Physiol 151:741–754

Ismayil A, Haxim Y, Wang Y, Li H, Qian L, Han T, Chen T, Jia Q, Yihao Liu A, Zhu S, Deng H, Gorovits R, Hong Y, Hanley-Bowdoin L, Liu Y (2018) Cotton Leaf Curl Multan virus C4 protein suppresses both transcriptional and post-transcriptional gene silencing by interacting with SAM synthetase. PLoS Pathog 29:e1007282

Kong X, Zhang C, Zheng H, Sun M, Zhang F, Zhang M, Cui F, Lv D, Liu L, Guo S, Zhang Y, Yuan X, Zhao S, Tian H, Ding Z (2020) Antagonistic interaction between auxin and SA signaling pathways regulates bacterial infection through lateral root in Arabidopsis. Cell Rep 25:108060

Krieger-Liszkay A, Trösch M, Krupinska K (2015) Generation of reactive oxygen species in thylakoids from senescing flag leaves of the barley varieties Lomerit and Carina. Planta 241:1497–1508

Kumar D, Hazra S, Datta R, Chattopadhyay S (2016) Transcriptome analysis of Arabidopsis mutants suggests a crosstalk between ABA, ethylene and GSH against combined cold and osmotic stress. Sci Rep 6:36867

La Camera S, L'haridon F, Astier J, Zander M, Abou-Mansour E, Page G, Thurow C, Wendehenne D, Gatz C, Métraux JP, Lamotte O (2011) The glutaredoxin AtGrxS13 is required to facilitate *Botrytis cinerea* infection of Arabidopsis thaliana plants. Plant J 68:507–519

Laemmli UK (1970) Cleavage of structural proteins during the assembly of the head of bacteriophage T4. Nature 227:680–685

Laporte D, Olate E, Salinas P, Salazar M, Jordana X, Holuigue L (2012) Glutaredoxin GRXS13 plays a key role in protection against photo-oxidative stress in Arabidopsis. J Exp Bot 63:503–515

Li F, Wang A (2019) RNA-targeted antiviral immunity: more than just RNA silencing. Trends Microbiol 27:792–805

Li N, Muthreich M, Huang LJ, Thurow C, Sun T, Zhang Y, Gatz C (2019) TGACG-BINDING FACTORs (TGAs) and TGA-interacting CC-type glutaredoxins modulate hyponastic growth in Arabidopsis thaliana. New Phytol 221:1906–1918

Li S, Ding H, Deng Y, Zhang J (2021) Knockdown of quinolinate phosphoribosyl transferase results in decreased salicylic acid-mediated pathogen resistance in *Arabidopsis thaliana*. Int J Mol Sci 22:8484

Lu Y (2018) Assembly and transfer of iron-sulfur clusters in the plastid. Front Plant Sci 9:336

Ma KW, Ma W (2016) Phytohormone pathways as targets of pathogens to facilitate infection. Plant Mol Biol 91:713–725

Malik WA, Wang X, Wangm X, Shu N, Cui R, Chen X, Wang D, Lu X, Yin Z, Wang J, Ye W (2020) Genome-wide expression analysis suggests glutaredoxin genes response to various stresses in cotton. Int J Biol Macromol 153:470–491

Marmonier A, Velt A, Villeroy C, Rustenholz C, Chesnais Q, Brault V (2022) Differential gene expression in aphids following virus acquisition from plants or from an artificial medium. BMC Genom 23:333

Millar AH, Sweetlove LJ, Giege P, Leaver CJ (2001) Analysis of the Arabidopsis mitochondrial proteome. Plant Physiol 127:1711–1727

Molina-Navarro MM, Casas C, Piedrafita L, Bellí G, Herrero E (2006) Prokaryotic and eukaryotic monothiol glutaredoxins are able to perform the functions of Grx5 in the biogenesis of Fe/S clusters in yeast mitochondria. FEBS Lett 580:2273–2280

Montes-Casado N, Tena F, Ramasamy S, Bonilla-Martínez A, Cebolla M, Pardo C, Montesinos C, García-Luque, I, Serra M (2010) In: La expresión constitutiva de una glutaredoxina (GRX) de *C. chinense* en plantas de Nicotiana benthamiana conlleva una reducción en la acumulación viral de PMMoV-I. Resúm. X Reunión de Biología Molecular de Plantas. Valencia. pág 175

Morita S, Yamashita Y, Fujiki M, Todaka R, Nishikawa Y, Hosoki A, Yabe C, Nakamura J, Kawamura K, Suwastika IN, Sato MH, Masumura T, Ogihara Y, Tanaka K, Satoh S (2015) Expression of a rice glutaredoxin in aleurone layers of developing and mature seeds: subcellular localization and possible functions in antioxidant defense. Planta 242:1195–1206

Ndamukong I, Abdallat AA, Thurow C, Fode B, Zander M, Weigel R, Gatz C (2007) SA-inducible Arabidopsis glutaredoxin interacts with TGA factors and suppresses JA-responsive PDF1.2 transcription. Plant J 50:128–139

Ning X, Sun Y, Wang C, Zhang W, Sun M, Hu H, Liu J, Yang L (2018) A Rice CPYC-Type Glutaredoxin OsGRX20 in protection against bacterial blight, methyl viologen and salt stresses. Front Plant Sci 9:111

Noctor G (2006) Metabolic signalling in defence and stress: the central roles of soluble redox couples. Plant Cell Environ 29:409–425

Obregón P, Martín R, Sanz A, Castresana C (2001) Activation of defence-related genes during senescence: a correlation between gene expression and cellular damage. Plant Mol Biol 46:67–77

Ogawa T, Muramoto K, Takada R, Nakagawa S, Shigeoka S, Yoshimura K (2016) Modulation of NADH levels by Arabidopsis Nudix Hydrolases, AtNUDX6 and 7, and the respective proteins themselves play distinct roles in the regulation of various cellular responses involved in biotic/abiotic stresses. Plant Cell Physiol 57:1295–1308

Palukaitis P, Yoon J-Y (2020) R gene mediated defense against viruse. Curr Opin Virol 45:1–7

Pavan Kumar BK, Kanakala S, Malathi VG, Gopal P, Usha R (2017) Transcriptomic and proteomic analysis of yellow mosaic diseased soybean. J Plant Biochem Biotechnol 26:224–234

Pétriacq P, de Bont L, Hager J, Didierlaurent L, Mauve C, Guérard F, Noctor G, Pelletier S, Renou J, Tcherkez G, Gakiére B (2012) Inducible NAD overproduction in Arabidopsis alters metabolic pools and gene expression correlated with increased salicylate content and resistance to Pst-AvrRpm1. Plant J 70:650–665

Pétriacq P, de Bont L, Tcherkez G, Gakière B (2013) NAD: not just a pawn on the board of plant-pathogen interactions. Plant Signal Behav 8:e22477

Pétriacq P, Ton J, Patrit O, Tcherkez G, Gakière B (2016) NAD acts as an integral regulator of multiple defense layers. Plant Physiol 172:1465–1479

Pre M, Atallah M, Champion A, de Vos M, Pieterse CMJ, Memelink J (2008) The AP2/ERF domain transcription factor ORA59 integrates jasmonic acid and ethylene signals in plant defense. Plant Physiol 147:1347–1357

Przybyla-Toscano J, Roland M, Gaymard F, Couturier J, Rouhier N (2018) Roles and maturation of iron–sulfur proteins in plastids. J Biol Inorg Chem 23:545–566

Robinson JB, Brent LG, Sumegi B, Srere PA (1987) An enzymatic approach to the study of the Krebs tricarboxylic acid cycle. In: Darley-Usmar WM, Rickwood D, Wilson MT (eds) Mitochondria: a practical approach. IRL Press, Oxford, pp 153–170

Rodriguez-Manzaneque MT, Ros J, Cabiscol E, Sorribas A, Herrero E (1999) Grx5 glutaredoxin plays a central role in protection against protein oxidative damage in Saccharomyces cerevisiae. Mol Cell Biol 19:8180–8190

Rodríguez-Manzaneque MT, Tamarit J, Bellí G, Ros J, Herrero E (2002) Grx5 is a mitochondrial glutaredoxin required for the activity of iron/sulfur clusters. Mol Biol Cell 13:1109–1121

Rouhier N, Unno H, Bandyopadhyay S, Masip L, Kim SK, Hirasawa M, Gualberto JM, Lattard V, Kusunoki M, Knaff DB, Georgiou G, Hase T, Johnson MK, Jacquot JP (2007) Functional, structural, and spectroscopic characterization of a glutathione-ligated [2Fe-2S] cluster in poplar glutaredoxin C1. Proc Natl Acad Sci USA 104:7379–7384

Ruan MB, Yang YL, Li K, Guo X, Wang B, Yu XL, Peng M (2018) Identification and characterization of drought-responsive CC-type glutaredoxins from cassava cultivars reveals their involvement in ABA signalling. BMC Plant Biol 18:329

Ruan M-B, Yu X-L, Guo X, Zhao P-J, Peng M (2022) Role of cassava CC-type glutaredoxin MeGRXC3 in regulating sensitivity to mannitol-induced osmotic stress dependent on its nuclear activity. BMC Plant Biol 22:41

Ruiz del Pino M, Moreno A, García de Lacoba M, Castillo-Lluva S, Gilardi P, SerraMT G-L (2003) Biological and molecular characterization of P101 isolate, a tobamoviral pepper strain from Bulgaria. Arch Virol 148:2115–2135

Sambrook J, Fritsch EF, Maniatis F (1989) Molecular cloning. A laboratory manual. Cold Spring Harbor Laboratory Press, New York

SAS Institute Inc (2004) What's New in SAS®9.0, 9.1, 9.1.2, and 9.1.3.Cary, NC: SAS Institute Inc.

Sharma R, Priya P, Jain M (2013) Modified expression of an auxin-responsive rice CC-type glutaredoxin gene affects multiple abiotic stress responses. Planta 238:871–884

Sidiq Y, Nakano M, Mori Y, Yaeno T (2021) Nicotinamide effectively suppresses Fusarium head blight in wheat plants. Int J Mol Sci 22:2968

Skopelitou K, Muleta AW, Pavli O, Skaracis GN, Flemetakis E, Papageorgiou AC, Labrou NE (2012) Overlapping protective roles for glutathione transferase gene family members in chemical and oxidative stress response in *Agrobacterium tumefaciens*. Funct Integr Genom 12:157–172

Stintzi A, Heitz T, Prasad V, Wiedemann-Merdinoglu S, Kauffmann S, Geoffroy P, Legrand M, Fritig B (1993) Plant 'pathogenesis-related' proteins and their role in defense against pathogens. Biochimie 75:687–706

Sun L, Ren H, Liu R, Li B, Wu T, Sun F, Liu H, Wang X, Dong H (2010) An h-type thioredoxin functions in tobacco defense responses to two species of viruses and an abiotic oxidative stress. Mol Plant Microbe Interact 23:1470–1485

Taiz L, Zeiger E (2010) Plant physiology, 5th edn. Sinauer Associates Inc., Sunderland

Uhrig JF, Huang LJ, Barghahn S, Willmer M, Thurow C, Gatz C (2017) CC-type glutaredoxins recruit the transcriptional co-repressor TOPLESS to TGA-dependent target promoters in Arabidopsis thaliana. Biochim Biophys Acta 1860:218–226

Van der Does D, Leon-Reyes A, Koornneef A, van Verk MC, Rodenburg N, Pauwels L, Goossens A, Körbes AP, Memelink J, Ritsema T, Van weesPierterse SCMCMJ (2013) Salicylic acid suppresses jasmonic acid signaling downstream of SCFCOI1-JAZ by targeting GCC promoter motifs via transcription factor ORA59. Plant Cell 25:744–761

Van der Zaal EJ, Memelink J, Mennes AM, Quint A, Libbenga KR (1987) Auxin-induced mRNA species in tobacco cell cultures. Plant Mol Biol 10:145–157
Van Loon LC, Van Strien EA (1999) The families of pathogenesis-related proteins, their activities, and comparative analysis ofPR-1 type proteins. Physiol Mol Plant Pathol 55:85–97
Van Loon LC, Rep M, Pieterse CM (2006) Significance of inducible defense-related proteins in infected plants. Annu Rev Phytopathol 44:135–162
Vieira Dos Santos C, Laugier E, Tarrago L, Massot V, Issakidis-Bourguet E, Rouhier N, Rey P (2007) Specificity of thioredoxins and glutaredoxins as electron donors to two distinct classes of Arabidopsis plastidial methionine sulfoxide reductases B. FEBS Lett 581:4371–4376
Vlot AC, Dempsey DA, Klessig DF (2009) Salicylic Acid, a multifaceted hormone to combat disease. Annu Rev Phytopathol 47:177–206
Wang D, Pajerowska-Mukhtar K, Culler AH, Dong X (2007) Salicylic acid inhibits pathogen growth in plants through repression of the auxin signaling pathway. Curr Biol 23:1784–1790
Wang Z, Xing S, Birkenbihl RP, Zachgo S (2009) Conserved functions of Arabidopsis and rice CC-type glutaredoxins in flower development and pathogen response. Mol Plant 2:323–335
Wang MB, Masuta C, Smith NA, Shimura H (2012) RNA silencing and plant viral diseases. Mol Plant Microbe Interact 25:1275–1285
Wang C, Zhang X, Mou Z (2016) Comparison of nicotinamide adenine dinucleotide phosphateinduced immune responses against biotrophic and necrotrophic pathogens in Arabidopsis thaliana. Plant Signal Behav 11:e1169358
Wang X, Jiang Z, Yue N, Jin X, Zhang X, Li Z, Zhang Y, Wang XB, Han C, Yu J, Li D (2021) Barley stripe mosaic virus γb protein disrupts chloroplast antioxidant defenses to optimize viral replication. EMBO J 16:e107660
Wasternack C, Hause B (2013) Jasmonates: biosynthesis, perception, signal transduction and action in plant stress response, growth and development. An update to the 2007 review in Annals of Botany. Annals Bot 111:1021–1058
Wetter C, Conti M, Altschuh D, Tabillion R, van Regenmortel MHV (1984) Pepper mild mottle virus, a tobamovirus infecting pepper cultivars in Sicily. Phytopathol 74:405–410
Wu Q, Lin J, Liu J-Z, Wang X, Lim W, Oh M, Park J, Rajashekar CB, Whitham SA, Cheng N-H, Hirschi KD, Park S (2012) Ectopic expression of Arabidopsis glutaredoxin AtGRXS17enhances thermotolerance in tomato. Plant Biotechnol J 10:945–955
WuQ YangJ, ChengN H-D, WhiteF-F ParkS (2017) Glutaredoxins in plant development, abiotic stress response, and iron homeostasis: from model organisms to crops. Environ Exp Bot 139:91–98
Xu Q, Ni H, Chen Q, Sun F, Zhou T, Lan Y, Zhou Y (2013) Comparative proteomic analysis reveals the cross-talk between the responses induced by H2O2 and by long-term Rice black-streaked dwarf virus infection in rice. PLoS ONE 8:e81640
Yang Y-X, Ahammed G, Wu C, Fan S, Zhou Y-H (2015) Crosstalk among jasmonate, salicylate and ethylene signaling pathways in plant disease and immune responses. Curr Protein Pept Sci Internat 16:450–461
Yang Y, Xue W, Chen P, Yuan X, Li X, Zhang T, Chen S (2021) Identification and expression analyzes of CC-type glutaredoxin in cucumber (*Cucumis sativus* L.) under abiotic stress. Sci Hortic 289:110417
Yang Y, Zhang X, Zhang L, Chen S (2022) CC-type glutaredoxin gene CsGRX4 in cucumber responds to *Botrytis cinerea* via JA signaling pathway. Sci Hortic 306:111440
Yuan HM, Liu WC, Lu YT (2017) CATALASE2 coordinates SA-mediated repression of both auxin accumulation and JA biosynthesis in plant defenses. Cell Host Microb 21:143–155
Zaffagnini M, Michelet L, Massot V, Trost P, Lemaire SD (2008) Biochemical characterization of glutaredoxins from *Chlamydomonas reinhardtii* reveals the unique properties of a chloroplastic CGFS-type glutaredoxin. J Biol Chem 283:8868–8876
Zaffagnini M, Bedhomme M, Marchand CH, Couturier JR, Gao XH, Rouhier N, Trost P, Lemaire SD (2012) Glutaredoxin S12: unique properties for redox signaling. Antioxid Redox Signal 16:17–32
Zander M, Chen S, Imkampe J, Thurow C, Gatz C (2012) Repression of the *Arabidopsis thaliana* jasmonic acid/ethylene induced defense pathway by TGA-interacting glutaredoxins depends on their C-terminal ALWL motif. Mol Plant 5:831–840
Zhang X, Mou Z (2009) Extracellular pyridine nucleotides induce PR gene expression and disease resistance in Arabidopsis. Plant J 57:302–312
Zhao Y, Liu M, He L, Li X, Wang F, Yan B, Wei J, Zhao C, Li Z, Xu J (2019) A cytosolic NAD+-dependent GPDH from maize (ZmGPDH1) is involved in conferring salt and osmotic stress tolerance. BMC Plant Biol 19:16
Zhao W, Zhou Y, Zhou X, Wang X, Ji Y (2021) Host GRXC6 restricts Tomato yellow leaf curl virus infection by inhibiting the nuclear export of the V2 protein. PLoS Pathog 17(8):e1009844

Authors and Affiliations

R. M. Saravana Kumar[1,2] · S. V. Ramesh[3] · Z. Sun[5] · Sugitha Thankappan[4] · Naga Prafulla Chandrika Nulu[6] · Asish Kanakaraj Binodh[7] · Sundaravelpandian Kalaipandian[2,6] · Ramachandran Srinivasan[8]

✉ R. M. Saravana Kumar
saravanakumarrm.sse@saveetha.com

S. V. Ramesh
ramesh.sv@icar.gov.in

Z. Sun
szc@cdmc.edu.cn

Naga Prafulla Chandrika Nulu
p.nulu@uq.edu.au

Asish Kanakaraj Binodh
asish@tnau.ac.in

Sundaravelpandian Kalaipandian
s.kalaipandian@uq.edu.au

Ramachandran Srinivasan
srini.vasan70@yahoo.com

[1] Department of Microbial and Plant Biotechnology, Centro de Investigaciones Biológicas Margarita Salas-CSIC, Madrid, Spain

[2] Department of Biotechnology, Saveetha School of Engineering, Saveetha Institute of Medical and Technical Sciences, Saveetha University, Chennai, Tamil Nadu 602105, India

[3] Physiology, Biochemistry and Post-Harvest Technology Division, ICAR-Central Plantation Crops Research Institute, Kasaragod, Kerala 671 124, India

[4] Department of Agriculture, School of Agriculture Sciences, Karunya Institute of Technology and Sciences, Karunya Nagar, Coimbatore, Tamil Nadu, India

[5] Sericultural Research Institute, Chengde Medical University, Chengde 067000, China

[6] School of Agriculture and Food Sustainability, The University of Queensland, Gatton, QLD 4343, Australia

[7] Center for Plant Breeding and Genetics, Tamil Nadu Agricultural University, Coimbatore, Tamil Nadu, India

[8] Centre for Ocean Research, Sathyabama Research Park, Sathyabama Institute of Science and Technology, Chennai 600119, Tamil Nadu, India